ACDC: The Adverse Conditions Dataset with Correspondences for Robust Semantic Driving Scene Perception

Christos Sakaridis*, Haoran Wang*, Ke Li, René Zurbrügg, Arpit Jadon, Wim Abbeloos, Daniel Olmeda Reino, Luc Van Gool, and Dengxin Dai

Abstract—Level-5 driving automation requires a robust visual perception system that can parse input images under *any* condition. However, existing driving datasets for dense semantic perception are either dominated by images captured under normal conditions or are small in scale. To address this, we introduce ACDC, the Adverse Conditions Dataset with Correspondences for training and testing methods for diverse semantic perception tasks on adverse visual conditions. ACDC consists of a large set of 8012 images, half of which (4006) are equally distributed between four common adverse conditions: fog, nighttime, rain, and snow. Each adverse-condition image comes with a high-quality pixel-level panoptic annotation, a corresponding image of the same scene under normal conditions, and a binary mask that distinguishes between intra-image regions of clear and uncertain semantic content. 1503 of the corresponding normal-condition images feature panoptic annotations, raising the total annotated images to 5509. ACDC supports the standard tasks of semantic segmentation, object detection, instance segmentation, and panoptic segmentation, as well as the newly introduced uncertainty-aware semantic segmentation. A detailed empirical study demonstrates the challenges that the adverse domains of ACDC pose to state-of-the-art supervised and unsupervised approaches and indicates the value of our dataset in steering future progress in the field. Our dataset and benchmark are publicly available at https://acdc.vision.ee.ethz.ch.

Index Terms—Driving dataset, robust perception, semantic segmentation, object detection, instance segmentation, panoptic segmentation, adverse conditions, autonomous cars, domain adaptation, unsupervised learning.

1 Introduction

Most of the prominent large-scale image-based datasets for driving scene perception, including Cityscapes [1], Vistas [2] and KITTI [3], are dominated by images captured under normal visual conditions, i.e., at daytime and in clear weather. Yet, vision applications such as automated driving impose a strict requirement on perception algorithms to maintain satisfactory performance in adverse domains. Although there have been efforts to include adverse visual domains in large-scale datasets, such as Oxford RobotCar [4] and BDD100K [5], these efforts focus either on localization/mapping tasks [4], [6] or on recognition tasks which *do not involve dense pixel-level outputs*, such as object detection [5], [7], [8]. For instance, while a notable 40% of the object detection set of BDD100K pertains to nighttime, only 3% of the images in its 10K semantic segmentation set, namely 345 images, are captured at nighttime [9]. In addition, the pixel-level annotation process for adverse-condition images is kept identical in [5], [10] to the normal-condition case, which leads to errors in the ground truth and renders it unreliable [9]. In contrast, seminal previous work [1] has underlined the need for *specialized* techniques and datasets for pixel-level semantic perception in adverse visual conditions, due to the inherent aleatory uncertainty in images captured in such conditions. These render entire image regions indiscernible even for humans.

ACDC constitutes a response to this need for a large-scale driving dataset specialized to adverse conditions, in terms of (i) size, (ii) domain adversity, and (iii) featured tasks. ACDC includes 5509 images with high-quality pixel-level panoptic annotations. From this complete set of images, 4006 images are distributed equally among four common adverse conditions in real-world driving environments, namely fog, nighttime, rain, and snow, and the rest 1503 pertain to normal conditions, i.e. daytime and clear weather, thus granting ACDC a scale that slightly exceeds that of Cityscapes. The adverse-condition part of the dataset was deliberately recorded with the respective adverse conditions clearly present. Thus, a large domain shift from the normal clear-weather daytime conditions was achieved. Moreover, for each adverse-condition image, a corresponding normal-condition image of the same scene from approximately the same viewpoint is provided, intended for use by weakly supervised methods.

As to the tasks that our dataset supports, apart from standard dense semantic perception tasks such semantic segmentation, object detection, instance segmentation and panoptic segmentation, we add the task of uncertainty-aware semantic segmentation. For the latter we introduce a specialized annotation protocol

- *C. Sakaridis, K. Li, and R. Zurbrügg are with the Department of Information Technology and Electrical Engineering, ETH Zürich, Switzerland.*
- *H. Wang, A. Jadon and D. Dai are with Max Planck Institute for Informatics, Saarland Informatics Campus, Germany.*
- *W. Abbeloos and D. Olmeda Reino are with Toyota Motor Europe, Belgium.*
- *L. Van Gool is with the Department of Information Technology and Electrical Engineering, ETH Zürich, Switzerland, with the Department of Electrical Engineering, KU Leuven, Belgium, and with INSAIT, Bulgaria.*
- *C. Sakaridis and H. Wang have contributed equally.*

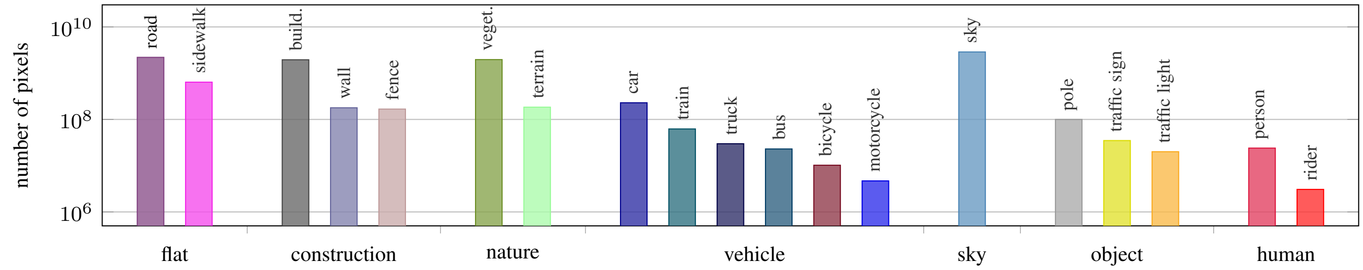

Fig. 1. Number of finely annotated pixels per class in ACDC.

and a dedicated performance metric, termed average uncertainty-aware IoU (AUIoU). The key characteristic of uncertainty-aware semantic segmentation is the principled inclusion of image regions with indiscernible semantic content—*invalid* regions—in annotation and evaluation. In particular, the annotation protocol for our adverse-condition images leverages privileged information in the form of the corresponding normal-condition images and the original adverse-condition videos, which enables to *reliably* assign legitimate semantic labels to invalid regions and to include them in the evaluation both for the aforementioned standard semantic perception tasks and for uncertainty-aware semantic segmentation. For the latter task, the separation of labeled pixels into invalid and valid is encoded in a binary mask. While both tasks require a hard semantic prediction, the uncertainty-aware task additionally expects a confidence map prediction. AUIoU is designed to take into account both the semantic and the confidence prediction and to reward predictions with low confidence on invalid pixels and high confidence on valid pixels. The requirement for an additional confidence prediction is relevant for safety-oriented applications, as it can help the downstream decision-making system avoid the fatal consequences of a low-confidence prediction being false, e.g. when a pedestrian is missed.

Apart from being a challenging benchmark for supervised semantic perception approaches, ACDC is a well-suited test bed for domain adaptation. A multitude of recent works have focused on unsupervised domain adaptation (UDA) for semantic segmentation [11], [12], [13], [14], [15], [16], [17], [18], [19], [20], [21], [22], [23], [24], [25], [26], [27] and object detection [28], [29], [30], [31], [32], [33], but most of them are validated only on artificial synthetic-to-real or real-to-synthetic settings, using GTA5 [34] and SYNTHIA [35] as source datasets and Cityscapes [1] as the target dataset for semantic segmentation and object detection or Cityscapes as the source dataset and Foggy Cityscapes [36] as the target dataset for object detection. The *real-world normal-to-adverse domain adaptation* scenario for semantic segmentation and object detection, which is much more relevant for real-world deployment of autonomous cars due to the difficulty of both acquiring and annotating adverse-condition data, has largely been overlooked. In particular, prior to the initial, conference version of ACDC [37], much fewer works had considered normal-to-adverse adaptation in their experiments [9], [36], [38], [39], [40], [41], [42] and whenever they did, they either restricted the target adverse domain to a single condition, e.g. nighttime [9], [39], [40], fog [36], [38], or rain [41], or did not include a quantitative evaluation on the real target domain altogether [42]. We attribute this fragmentation of normal-to-adverse adaptation works to the absence of a general large-scale dataset for semantic perception that evenly covers the majority of common adverse conditions and provides reliable ground truth for a sound evaluation in such challenging domains. ACDC answers exactly the need for such a dataset and has already served since its initial release as a test bed for unsupervised and weakly supervised domain adaptation [30], [43], [44], [45], [46], [47], [48]. Experiments such as Cityscapes→ACDC adaptation are straightforward thanks to the identical label sets of the two datasets, which facilitates validation of new domain adaptation approaches in the normal-to-adverse setting. We further introduce a novel domain adaptation setting from Cityscapes to the normal-condition part of ACDC, which isolates the sensor-level shift as the only difference in source and target domains given the geographical similarity of the two datasets, and establish a new UDA benchmark based on this setting.

Overall, we experiment with ACDC on all five semantic perception tasks it supports in four main directions: (i) unsupervised and weakly supervised normal-to-adverse and sensor-level domain adaptation, (ii) supervised semantic perception in adverse conditions, (iii) evaluation of models externally pre-trained on normal conditions, and (iv) evaluation of uncertainty-aware semantic segmentation baselines and oracles. Results show that access to ground-truth annotations under adverse conditions is indispensable for achieving high performance, as pre-trained models severely deteriorate under adverse conditions. Moreover, the real-world Cityscapes→ACDC adaptation scenario stands for a challenging setting for all state-of-the-art UDA methods, which still trail fully supervised counterparts. This underlines the need for UDA methods that perform better when handling adverse target domains and highlights the importance of ACDC in steering future work in this direction. Finally, the uncertainty-aware annotations of ACDC create significant room for improvement over simple confidence prediction baselines and help promote future work on semantic segmentation methods that simultaneously models uncertainty.

An earlier version of this work has appeared in the International Conference on Computer Vision [37]. Compared to the conference version, this paper makes the following additional contributions:

1) A substantial amount of new annotations to the dataset, including (i) the upgrade of the initial 4006 semantic segmentation annotations of the adverse-condition images of ACDC to panoptic segmentation annotations and (ii) the annotation of 1503 normal-condition images, which were not annotated at all in the conference version, for panoptic segmentation.
2) An extensive set of experimental comparisons on the newly supported tasks compared to the conference version, i.e. object detection, instance segmentation, and panoptic segmentation, covering diverse settings such as normal-to-adverse domain adaptation, sensor-level domain adaptation, supervised

learning on adverse conditions, and evaluation of models externally pre-trained on normal conditions.

3) An updated set of experimental comparisons on tasks and settings, such as normal-to-adverse domain adaptation for semantic segmentation and supervised semantic segmentation, which were already included in the conference version, taking into account respective recent state-of-the-art methods that have been presented since the publication of the conference version.
4) Other enhanced and updated parts, such as (i) additional statistics and comparisons for dataset annotations based on the new format and the increased scale of the annotations, and (ii) an extended and updated overview of the related work, which covers the newly supported tasks and the latest advances in driving datasets for semantic perception and in adaptation of semantic segmentation.

2 Related Work

Datasets for driving scene perception include real-world and synthetic sets that support geometric and recognition tasks. KITTI [3] and Cityscapes [1] pioneered this area with LiDAR and semantic image annotations, respectively. Subsequent datasets mostly aimed at increasing the scale [49], diversity [2] and number of tasks [5]. As high-quality pixel-level annotations proved hard to acquire [1], [2], another line of work focused on creating synthetic sets at an even larger scale [34], [35], [50], [51], [52] and in which ground truth is automatically generated, as well as translating real datasets to adverse conditions such as fog or rain [36], [38], [53]. Oxford Robotcar [4] was the first real-world large-scale dataset in which adverse visual conditions such as nighttime, rain and snow were significantly represented, but it did not feature semantic annotations. While more recent large-scale sets [54], [55] that cover adverse conditions, such as Waymo Open [7] and nuScenes [8], include bounding boxes, they still lack dense pixel-level semantic annotations, which are vital for real-world autonomous agents [56]. BDD100K [5] was the only exception to this rule prior to the publication of the conference version [37] of this paper, with ca. 13% of its 10000 pixel-level annotations pertaining to adverse conditions but containing severe errors [9]. At the same time, only a small portion of each of the 1881 adverse-condition images in ADUULM [57] is annotated. On the other hand, several sets with small-scale pixel-level annotations covering adverse conditions [10] had been presented, focusing on fog [36], [58], nighttime [9], [39], and rain [59]. A notable case is Dark Zurich [9], with 201 fine pixel-level nighttime annotations and a dedicated annotation protocol and evaluation metric that handles regions with ambiguous content. The initial, conference version of ACDC improved both upon BDD100K, in terms of ground truth quality, and Dark Zurich, in terms of scale and condition diversity, featuring 5509 high-quality fine instance-level semantic annotations in which fog, night, rain, snow, and normal conditions are evenly represented. Since the initial publication of ACDC, a larger-scale version of WildDash, namely Wilddash2 [60], has been released. The present extended version of ACDC exceeds the scale of Wilddash2 annotations (5509 vs. 5000). Moreover, in contrast both to Wilddash2 and to other recent dense semantic perception datasets with adverse conditions [61], [62], ACDC features cross-condition image-level correspondences with normal-condition reference images as well as a specialized annotation protocol which hinges exactly on the aforementioned correspondences to allow the assignment of legitimate, reliable semantic labels to indiscernible image regions which would otherwise be impossible to label.

Semantic segmentation has progressed rapidly over the last years, primarily through the design of convolutional neural networks. Based on fully convolutional architectures [63], seminal works introduced atrous convolution [64], [65], [66] and encoder-decoder structures with skip connections [67] to exploit context and improve localization, respectively. Balancing between global and local information was further addressed by parallel branches of different resolutions [68], [69] and global pooling [70]. Other works focused on real-time performance [71], leveraging different modalities such as depth [72], and defining neighborhood-based supervision [73] for segmentation. The current state of the art includes i.a. DeepLabv3+ [74] and ANN [75] with pyramid pooling modules, DANet [76] and CCNet [77] with attention mechanisms, and HRNet [78] and OCR [79] with high-resolution representations. While performance on the popular Cityscapes benchmark is increasingly saturating, we demonstrate that state-of-the-art methods achieve much lower performance on ACDC (see Sec. 6.1). Thus, ACDC provides a more challenging benchmark for semantic segmentation thanks to the adversity of its domains and is therefore able to foster further progress in the field.

Adaptation of semantic segmentation networks to domains where full supervision is not available was launched shortly after the introduction of supervised approaches [80]. A major class of UDA works has employed adversarial domain adaptation to implicitly align the source and target domains at the level of pixels and/or features [12], [13], [14], [15], [16], [19], [20], [22], [26], [38], [81]. Other approaches to UDA have relied on self-training with pseudo-labels in the target domain [18], [23], [82], [83], [84], [85] or have combined self-training with adversarial adaptation [21] or with pixel-level adaptation via explicit transforms from source to target [24], [25]. However, all aforementioned approaches have been evaluated only on the artificial scenario of synthetic-to-real adaptation and overlook *normal-to-adverse adaptation*, which is of higher practical importance for autonomous cars. ACDC has constituted the large-scale target-domain dataset which had previously been missing for such a normal-to-adverse experiment and steered the development of unsupervised and weakly supervised adaptation approaches [30], [43], [44], [45], [46], [47], [48] that can cope with adverse target domains via the introduction of a competitive normal-to-adverse adaptation benchmark since the conference version of this paper [37]. In the present extended version, we additionally introduce a sensor-level adaptation benchmark from Cityscapes to the newly annotated normal-condition split of ACDC. This benchmark does not involve a condition-level shift between the source and target domain, which both pertain to normal conditions, but it instead features a change in the camera sensor from Cityscapes to ACDC, which induces a sensor-related real-to-real low-level shift in the input images.

Instance segmentation and panoptic segmentation distinguish instances in the images compared to the semantic segmentation task. Instance segmentation aims to assign a segmentation mask for each object of interest in the image, while panoptic segmentation task encompasses masks for both stuff and things classes as the combination of semantic segmentation and instance segmentation. Both of these two tasks are applied in various

(a) Input image I (b) Stage 1 annotation (draft) (c) Corresponding image I' (d) Stage 2 annotation (GT) (e) Invalid mask J

Fig. 2. **Illustration of semantic annotation protocol for ACDC.** The color coding of the semantic classes matches Fig. 1. All annotations in (b), (d) and (e) pertain to the input image I in (a). A white color in (b) and (d) denotes unlabeled pixels.

real-world applications like robotics, healthcare and geoscience. For instance segmentation, many works either follow the detect-then-segment pipeline [86] or explore to generate a dynamic number of instance masks directly with clustering or dynamic kernels. The pioneering work, Mask R-CNN generate instance masks based on object bounding box proposals. The following specialized instance segmentation works like Cascaded Mask R-CNN, HTC and Detectors mainly work on extracting better feature representations and generating more accurate object proposals. For panoptic segmentation, early works strive to combine semantic segmentation models and instance segmentation models to predict unified panoptic masks. Recent works begin to view the panoptic segmentation task in a unified perspective and formulate the stuff and things segmentation as a set prediction problem. The current state of the art for panoptic segmentation includes i.a. PanopticFPN and Panoptic-Deeplab with specialized instance prediction branches and semantic prediction branches, K-Net with dynamic kernels, and MaskFormer and Mask2Former with transformer architecture. Although current instance segmentation and panoptic segmentation models obtains impressive improvement on the popular Cityscapes benchmark, we present that these state-of-the-art generalize poorly to ACDC. The adverse images in ACDC poses a new challenges for instance segmentation models and panoptic segmentation models and would be able to further encourage the development in the fields.

Adaptation of object detection networks from a labeled source domain to another unlabeled target domain is also an active research field. Currently, there are mainly two categories of UDA for object detection methods: domain alignment and self-training. Domain alignment strive to bridge the domain gap by minimizing the domain discrepancy through style transfer, adversarial training and graph matching. Self-training relies on pseudo labels to extract rich knowledge contained in target domain and presents promising performance. Although all aforementioned have been proven effective in alleviating the damage of domain shifts, due to the lack of dataset with rich adverse conditions, these methods are mainly evaluated on synthetic-to-real, cross-city and cross-camera settings. The *normal-to-adverse adaptation*, which is of high value for intelligent driving systems, is rarely discussed. ACDC provides a large-scale data in adverse conditions and would promote the progress of unsupervised and weakly supervised object detection methods for adverse conditions.

3 ACDC Dataset

We base the design of ACDC on the same general principles as seminal normal-condition datasets [1] and adapt the collection and annotation process to fit better the adverse condition setting at hand.

3.1 Collection

Our data collection is guided by the decision to record the same set of scenes both under adverse and normal conditions. We define the domain of *normal* conditions as the combination of daytime and clear weather, i.e. good visibility and no precipitation or snow cover on the ground. While the focus of ACDC is on adverse conditions, the acquisition of the corresponding normal-condition images is vital both for the subsequent annotation step and to support weakly supervised methods, as the same scene can be much easier to parse in normal conditions, both for humans and machines.

Thus, we recorded several days of video in Switzerland by driving around in a car, primarily in urban areas but also on highways and in rural regions. In order to have a clear domain separation between different adverse conditions, we use the following criterion for the adverse-condition recordings: each recording takes place under only one type of adversity from a set of four items, i.e., fog, nighttime, rain, and snow. For example, our foggy recordings are performed at daytime and without rain or snow. For snow, both snowfall and snow cover on the ground are admissible. Moreover, we keep for further processing only the parts of the adverse-condition recordings that correspond to an intense presence of the respective condition, so as to maximize the domain shift from normal conditions as well as domain adversity.

We record with a 1080p GoPro Hero 5 camera, mounted in front of the windshield at nighttime and in normal conditions and behind the windshield in fog, rain, and snow. The camera records 8-bit RGB frames at a rate of 30 Hz.

3.2 Correspondence Establishment

Our camera also provides GPS readings, which allow us to establish *image-level correspondences* between adverse-condition and normal-condition recordings. In particular, for each adverse-condition recording, we perform a normal-condition recording along exactly the same route. We then use the sequences of GPS measurements of the two recordings to perform a global dynamic-programming-based matching of the adverse GPS sequence to the normal one, where the objective is defined by the Euclidean distances of matched pairs of GPS samples. Our global matching handles routes with loops better than simple nearest neighbors. Each adverse-condition frame is then matched to a normal-condition frame based on the corresponding matched samples of the GPS sequences.

3.3 Dataset Splits

ACDC is split into four sets corresponding to the examined conditions. We manually selected 1000 foggy, 1006 nighttime, 1000 rainy and 1000 snowy images from the recordings for dense pixel-level semantic annotation, for a total of 4006 adverse-condition images. The selection process aimed at maximizing the complexity and diversity of captured scenes. Within each recording, any pair of selected images is at least 20 s or 50 m apart (whatever comes first).

The dataset is also split into training, validation, and test sets. We apply a global geographical split across all conditions, so that there is zero overlap between the three sets, even for different conditions. Given the abundance of training data from normal-condition datasets [1], [2], [5] that allow to pre-train semantic segmentation models, we opt for a split with a greater test set size than usual. This aims at providing a highly challenging benchmark for semantic segmentation, both in terms of scale and domain adversity. In particular, we split the set of each adverse condition into 400 training, 100 validation and 500 test images, except the nighttime set with 106 validation images. This results in a total of 1600 training and 406 validation images with public annotations and 2000 test images with annotations withheld for benchmarking purposes, as per standard practice [1].

In the present extended version of ACDC, we newly provide annotations for a subset of the 4006 corresponding normal-condition reference images of the dataset, all of which were not annotated in the initial conference version. More specifically, for the reference normal-condition sets corresponding to each of the four adverse conditions, we annotate 50% of the training splits (corresponding to 200 images each) and of the validation splits (corresponding to 50 images for the fog, rain, and snow reference validation splits and 53 images for the nighttime reference validation split) and 25% of the test splits (corresponding to 125 images each). This results in a total of 800 training and 203 validation normal-condition reference images with public annotations and 500 test normal-condition reference images with annotations withheld for benchmarking purposes, as explained above. Added to the 4006 adverse-condition annotations of the initial conference version, these 1503 new normal-condition annotations raise the overall scale of annotations of the extended version of ACDC to 5509 pixel-level annotations.

3.4 Semantic Annotation

Images captured under adverse conditions contain invalid regions, i.e. regions with indiscernible semantic content, which generally co-exist with valid regions in the same image. We take this into account for creating annotations of ACDC and design a specialized annotation protocol, which leverages privileged information from the corresponding normal-condition images and the original adverse-condition videos and allows (i) the reliable assignment of semantic labels to invalid regions and (ii) the creation of a binary mask that distinguishes valid from invalid regions.

Our annotation protocol for the 4006 adverse-condition images consists of two cascaded annotation stages. At stage 1, a semantic labeling draft is manually produced from the adverse-condition image I, in which pixels that cannot be unquestionably assigned to a single semantic class are left unlabeled. At stage 2, the corresponding normal-condition image I' and the adverse-condition video from which I was extracted are used to augment and finalize the annotation. In particular, the annotator can assign a legitimate label to pixels that were left unlabeled in stage 1 and correct pixels that were incorrectly labeled in stage 1. Pixels that remain unclear in stage 2 are left unlabeled and are not used for training or evaluation.

The final annotation outputs are twofold: (i) the final semantic annotation H after stage 2, and (ii) a binary invalid mask J, where

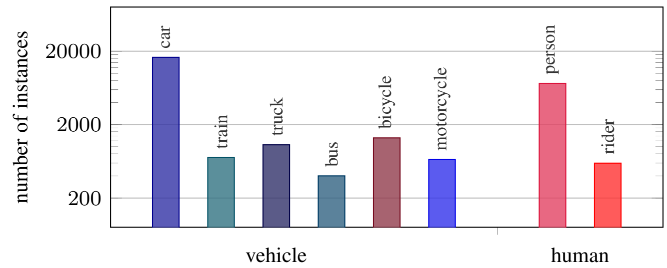

Fig. 3. Number of instances per class in ACDC.

pixels whose label changed from stage 1 to stage 2 are set to 1 (invalid) and pixels with the same semantic label for both stages are set to 0 (valid). J enables the introduction of the new task of uncertainty-aware semantic segmentation, which we detail in Sec. 8.

The 4006 fine pixel-level annotations of ACDC were created by a professional team of annotators to ensure high-quality ground truth. Annotators were asked to be conservative in labeling pixels in both stages, so as to minimize errors. Both the initial draft from stage 1 and the final annotation from stage 2 passed through quality control. The total time required for annotating a single adverse-condition image was 3.3 h on average. The semantic annotation of the 1503 normal-condition images is conducted in the standard way by using only the input normal-condition image.

The class specifications of ACDC are directly inherited from Cityscapes. In particular, we annotate the 19 evaluation classes of Cityscapes, which include the most common and traffic-related objects in driving scenes. Objects that belong to classes outside this set receive a fall-back label and are not used for training or evaluation. This choice of classes provides full compatibility of ACDC to Cityscapes and other normal-condition datasets for semantic segmentation [2], [5]. Detailed annotation statistics are presented in Fig. 1. An example of our two-stage annotation protocol is shown in Fig. 2 for a snowy image. Note the assignment of a region in the lower right part of the image that is unlabeled at stage 1 (Fig. 2b) to the *road* label at stage 2 (Fig. 2d), thanks to the clear view from the normal-condition image.

3.5 Instance Annotation

Besides the pixel-level semantic annotations, in the present extended version we also create dense instance-level annotations for countable objects, including vehicles and humans, to support higher-level semantic perception tasks such as instance segmentation and panoptic segmentation. To fully utilize the semantic annotations and ensure the consistency between different annotations, we develop a protocol to generate instance-level annotations based on semantic masks.

Our instance annotation protocol contains two steps. In the first step, we convert the pixel-level semantic masks to polygon representations. In the second step, we ask the annotators to merge/split polygons to form polygon annotation for each instance. The polygon annotations are finally transformed to standard COCO format for instance-level tasks. The instance-level annotations were also combined with prior semantic annotations to construct panoptic annotations for panoptic segmentation.

The total 4006 adverse-condition images and 1503 normal-condition reference images are annotated at the instance level by a professional team of annotators. Each final annotation is checked by at least two annotators and passed through quality control. The

TABLE 1
Comparison of ACDC against prior adverse-condition semantic segmentation datasets. "Adverse annot.": total annotated adverse-condition images, "Fog"/"Night"/"Rain"/"Snow": annotated foggy/nighttime/rainy/snowy images, "Inv. regions": can invalid regions get legitimate labels?, "Corr. normal": are corresponding normal-condition images available?, "Inv. masks": are invalid masks available?

Dataset	Adverse annot.	Fog	Night	Rain	Snow	Classes	Reliable GT	Fine GT	Inv. regions	Corr. normal	Inv. masks
Foggy Driving [36]	101	101	0	0	0	19	✓	✓	×	×	×
Foggy Zurich [58]	40	40	0	0	0	19	✓	✓	×	×	×
Nighttime Driving [39]	50	0	50	0	0	19	✓	×	×	×	×
Dark Zurich [9]	201	0	201	0	0	19	✓	✓	✓	✓	✓
Raincouver [59]	326	0	95	326	0	3	✓	×	×	×	×
WildDash [10]	226	10	13	13	26	19	✓	✓	×	×	×
BDD100K [5]	1346	23	345	213	765	19	×	✓	×	×	×
ACDC	**4006**	**1000**	**1006**	**1000**	**1000**	19	✓	✓	✓	✓	✓

TABLE 2
Absolute and average number of instances in adverse conditions for ACDC, BDD100K, and DAWN on the respective training and validation datasets. ACDC (all) includes all training, validation and testing set.

	#humans[10^3]	#vehicles[10^3]	#h/image	#v/image
ACDC	2.5	10.4	1.2	5.2
ACDC (all)	7.9	20.7	1.9	5.1
BDD100K [5]	0.7	6.6	1.1	10.2
DAWN [87]	0.4	7.4	0.4	7.4

total time required for annotating a single image given the initial semantic mask was 0.6 h on average.

To be compatible with semantic annotations, for instance annotations, we only create instance-level masks for traffic participant classes such as humans and vehicles. We present the detailed distribution of instances in ACDC in Fig. 3. The dataset follows a long-tail distribution across countable classes in terms of instance counts. The *vehicle* category is dominated by the *car* class, while the *person* class emerges as the predominant class for the *human* category. This skewed distribution reflects the real world, where cars often outnumber other vehicle types heavily, and pedestrians are more commonly encountered compared to riders.

3.6 Comparison to Related Datasets

To the best of our knowledge, ACDC constitutes the largest adverse-condition driving dataset for dense semantic perception to date. In Table 1, we compare ACDC to prior datasets that also address semantic segmentation under adverse conditions. Most of these datasets focus on a single condition and are of small scale. WildDash covers a wider variety of adverse conditions but also has a small scale. BDD100K includes 10000 images with semantic segmentation annotations. We inspected these images manually to identify those that pertain to fog, night, rain, and snow. We found that only 1346/10000 images pertain to any of these four conditions. By contrast, ACDC is primarily composed of these four common adverse conditions. Notably, it contains one order of magnitude more annotated images than any other competing dataset for each of fog, night and rain. At the same time, our specialized annotation protocol using corresponding normal-condition images ensures *reliable* annotations even for invalid regions, making ACDC a high-quality dataset for training and evaluation for adverse conditions. We also provide a comparison on the number of annotated instances with existing datasets covering adverse conditions in Table 2. Only a small portion of BDD100K provides instance-level annotations in adverse conditions including fog, night, rain and snow. The DAWN dataset consists of 1000 images in adverse weather conditions from real traffic environments. ACDC presents clear advantages in the total number of annotated humans and vehicles in challenging adverse conditions, thereby offering a broader spectrum of diverse scenes under challenging adverse conditions.

4 Normal-to-Adverse Adaptation

ACDC supports various semantic perception tasks, including semantic segmentation, object detection, instance segmentation, and panoptic segmentation. In this section, we experiment on our dataset with domain adaptation methods for semantic segmentation and object detection.

4.1 Domain-Adaptive Semantic Segmentation

We present a new benchmark for UDA of semantic segmentation: Cityscapes→ACDC. We select fourteen representative state-of-the-art UDA methods, train them with their default configurations for adaptation from Cityscapes to the entire ACDC and present the results in Table 3. Ten of these methods are trained with the earlier DeepLabv2-based architecture [65], while five of these methods are trained with the more modern SegFormer backbone [88]. While most of the DeepLabv2-based methods have previously achieved significant performance gains in the popular synthetic-to-real adaptation setting, we observe that most of them do not improve upon the source-domain baseline in our normal-to-adverse setting. The best-performing DeepLabv2-based methods are CISS and FDA, which are respectively based on non-adversarial, feature-level and pixel-level adaptation strategies with an explicit Fourier prior. Only CISS slightly outperforms the model that is supervised with only 100 target-domain labels. With regard to the more recent, SegFormer-based methods, most of them manage to deliver substantial performance improvements on the target, adverse-condition domain of ACDC compared to the already strong source model. In fact, MIC, CISS, and HRDA even prove capable of *surpassing* the performance of the *oracle* model, which has exactly the same architecture as the source model but also access to target-domain labels during training. This is an encouraging finding for the domain adaptation community, as it corroborates the benefit of introducing informed inductive biases to learned models via proper losses or architectural modules in order to improve their generalization to unlabeled data over merely feeding the models with more labeled data.

TABLE 3
Comparison of state-of-the-art domain-adaptive semantic segmentation methods on Cityscapes→ACDC adaptation. Cityscapes serves as the source domain and the entire adverse-condition part of ACDC including all four adverse conditions serves as the target domain. The first, second, and third groups of rows present unsupervised DeepLabv2-based [65], weakly supervised, and unsupervised SegFormer-based [88] methods, respectively. The performance of the respective models trained on Cityscapes (Source model) and of the oracle models trained on ACDC with all 1600 labels (Oracle) is also reported in all cases, while for the DeepLabv2 case, we additionally report the performance of the partial oracle models trained on ACDC with 100 labels (Oracle-100), and 200 labels (Oracle-200).

Method	road	sidew.	build.	wall	fence	pole	light	sign	veget.	terrain	sky	person	rider	car	truck	bus	train	motorc.	bicycle	mIoU
Source model [65]	71.9	26.2	51.1	18.8	22.5	19.7	33.0	27.7	67.9	28.6	44.2	43.1	22.1	71.2	29.8	33.3	48.4	26.2	35.8	38.0
AdaptSegNet [15]	69.4	34.0	52.8	13.5	18.0	4.3	14.9	9.7	64.0	23.1	38.2	38.6	20.1	59.3	35.6	30.6	53.9	19.8	33.9	33.4
ADVENT [19]	72.9	14.3	40.5	16.6	21.2	9.3	17.4	21.2	63.8	23.8	18.3	32.6	19.5	69.5	36.2	34.5	46.2	26.9	36.1	32.7
BDL [21]	56.0	32.5	68.1	20.1	17.4	15.8	30.2	28.7	59.9	25.3	37.7	28.7	25.5	70.2	39.6	40.5	52.7	29.2	38.4	37.7
CLAN [20]	79.1	29.5	45.9	18.1	21.3	22.1	35.3	40.7	67.4	29.4	32.8	42.7	18.5	73.6	42.0	31.6	55.7	25.4	30.7	39.0
CRST [23]	51.7	24.4	67.8	13.3	9.7	30.2	38.2	34.1	58.0	25.2	76.8	39.9	17.1	65.4	3.7	6.6	39.6	11.8	8.6	32.8
FDA [24]	73.2	34.7	59.0	24.8	29.5	28.6	43.3	44.9	70.1	28.2	54.7	47.0	28.5	74.6	44.8	52.3	63.3	28.3	39.5	45.7
SIM [26]	53.8	6.8	75.5	11.6	22.3	11.7	23.4	25.7	66.1	8.3	80.6	41.8	24.8	49.7	38.6	21.0	41.8	25.1	29.6	34.6
MRNet [27]	72.2	8.2	36.4	13.7	18.5	20.4	38.7	45.4	70.2	35.7	5.0	47.8	19.1	73.6	42.1	36.0	47.4	17.7	37.4	36.1
DACS [89]	58.5	34.7	76.4	20.9	22.6	31.7	32.7	46.8	58.7	39.0	36.3	43.7	20.5	72.3	39.6	34.8	51.1	24.6	38.2	41.2
CISS [46]	70.5	36.7	67.0	29.4	30.2	31.6	45.6	48.9	70.4	24.7	65.5	48.2	31.1	76.6	45.7	47.0	62.8	26.8	38.9	47.2
Oracle-100	84.4	54.8	76.4	19.3	28.9	29.5	36.5	42.6	74.2	40.3	87.7	42.5	16.5	74.9	36.5	28.6	55.9	27.3	38.6	47.1
Oracle-200	86.2	55.0	77.9	21.7	30.9	30.0	37.6	42.5	76.8	45.8	90.2	45.4	19.1	75.8	38.5	38.0	64.2	21.6	39.5	49.3
Oracle	88.0	62.3	80.8	37.0	35.1	33.9	49.8	49.5	80.1	50.7	92.5	51.1	26.5	79.9	49.0	41.1	72.2	26.5	44.2	55.3
Source model [68]	66.3	28.9	67.6	19.2	25.9	36.7	50.0	47.5	69.4	28.8	83.0	42.1	17.7	72.6	30.9	31.6	48.9	26.1	36.7	43.7
MGCDA [9]	73.4	28.7	69.9	19.3	26.3	36.8	53.0	53.3	75.4	32.0	84.6	51.0	26.1	77.6	43.2	45.9	53.9	32.7	41.5	48.7
Oracle	92.5	71.2	86.2	39.0	44.0	53.2	68.8	66.0	85.1	59.3	94.9	65.2	38.5	85.8	53.8	59.7	76.2	47.5	54.5	65.3
Source model [43]	80.5	37.4	80.5	34.7	30.4	43.7	57.9	54.2	79.0	51.6	87.6	57.4	34.0	81.5	51.9	59.1	70.4	37.5	49.3	56.8
DAFormer [43]	58.4	51.3	84.0	42.7	35.1	50.7	30.0	57.0	74.8	52.8	51.3	58.2	32.6	82.7	58.3	54.9	82.4	44.1	50.7	55.4
SePiCo [44]	61.3	48.6	84.9	39.6	40.3	54.2	48.9	60.6	74.8	54.3	57.2	65.2	38.3	84.8	66.2	60.4	85.5	44.5	53.1	59.1
HRDA [45]	88.3	57.9	88.1	55.2	36.7	56.3	62.9	65.3	74.2	57.7	85.9	68.8	45.6	88.5	76.4	82.4	87.7	52.7	60.4	68.0
CISS [46]	92.0	69.6	89.2	57.2	40.5	55.8	67.1	67.3	75.2	59.7	86.4	70.0	47.5	88.9	73.1	77.5	87.0	55.6	61.7	69.6
MIC [30]	90.8	67.1	89.2	54.5	40.5	57.2	62.0	68.4	76.3	61.8	87.0	71.3	49.4	89.7	75.7	86.8	89.1	56.9	63.0	70.4
Oracle	93.2	74.2	89.5	54.5	47.4	57.0	68.9	66.9	88.5	66.0	96.2	64.2	30.6	85.8	59.6	64.7	86.3	39.8	54.3	67.8

TABLE 4
Comparison of state-of-the-art unsupervised domain adaptation methods on Cityscapes→ACDC adaptation for individual conditions. We train a separate model on each condition-specific subset of ACDC and evaluate each model on the condition it has been trained for. Performance of the model trained only on the source domain (Source model) and of oracles with access to the target-domain labels for each condition (Oracle) is also reported.

Method	Fog	Night	Rain	Snow
Source model	33.5	30.1	44.5	40.2
AdaptSegNet [15]	31.8	29.7	49.0	35.3
ADVENT [19]	32.9	31.7	44.3	32.1
BDL [21]	37.7	33.8	49.7	36.4
CLAN [20]	39.0	31.6	44.0	37.7
FDA [24]	39.5	37.1	53.3	46.9
SIM [26]	36.6	28.0	44.5	33.3
MRNet [27]	38.8	27.9	45.4	38.7
Oracle	52.2	45.4	57.6	56.8

The image-level correspondences of ACDC between adverse and normal conditions act as weak supervision. We thus additionally experiment with MGCDA, a weakly supervised method that exploits such correspondences. MGCDA outperforms FDA but is still inferior to its fully supervised counterpart.

In addition, we train state-of-the-art UDA methods to adapt from Cityscapes to individual conditions of ACDC in Table 4. The increased uniformity of the target domains in this setting results in larger performance gains overall compared to Table 3. However, night and snow prove particularly challenging for most methods and only FDA brings a performance gain on snow.

4.2 Domain-Adaptive Object Detection

We establish a new benchmark for UDA of object detection: Cityscapes→ACDC. We select seven representative UDA methods for detection, and perform adaptation from Cityscapes to the entire adverse-condition part of the ACDC training set including all four adverse conditions, with the default configuration designed for Cityscapes to Foggy Cityscapes adaptation. The Cityscapes→ACDC adaptation results are reported in Table 5. As different UDA methods are built on either one-stage or two-stage detection frameworks, we report the results in two groups: two-stage UDA detection methods share the same Faster R-CNN detection architecture and one-stage UDA detection methods share the same FCOS detection framework. For two-stage detection methods, we report the performance of the adversarial-training-based UDA methods DA-Faster, SADA and MIC (SADA) and the graph-matching-based method FRCNN-SIGMA++. For one-stage detection methods, we present the results of the adversarial-learning-based method EPM and the graph-matching-based method SIGMA. Following the previous works in cross-domain object detection, we report AP_{50}^{box} for each category by default. We also provide overall COCO AP^{box} for reference. As most of UDA object detection works benchmark their method on Cityscapes to Foggy Cityscapes for normal-to-adverse adaptation, for comparison we adopt the same configurations to perform adaptation from Cityscapes to ACDC. We expect to present the difference between real and synthetic adverse data and the

TABLE 5
Comparison of state-of-the-art domain-adaptive object detection methods on Cityscapes→ACDC adaptation. Cityscapes serves as the source domain and the entire adverse-condition part of ACDC including all four adverse conditions serves as the target domain. The first and second groups of rows present unsupervised and weakly supervised methods, respectively. All unsupervised methods share the same network architecture. The performance of the respective models trained on Cityscapes (Source model) and of the oracle models trained on ACDC with all 1600 labels (Oracle) is also reported.

Method	person	rider	car	truck	bus	train	motorc.	bicycle	AP_{50}^{box}	AP^{box}
Source model (Faster R-CNN) [90]	22.8	12.2	51.9	20.0	19.6	16.0	13.4	10.4	20.8	10.3
DA-Faster [28]	28.0	13.6	57.0	13.1	13.3	10.6	8.2	14.2	19.8	9.2
SADA [29]	34.2	12.2	61.8	11.0	5.4	7.3	9.6	15.8	19.7	9.4
MIC (SADA) [30]	40.0	23.0	67.2	13.5	8.2	12.3	20.5	22.9	25.9	12.1
FRCNN-SIGMA++ [31]	26.4	19.5	13.6	16.5	16.6	57.8	22.7	20.5	24.2	11.9
Oracle	28.7	17.3	61.8	29.8	14.8	36.1	19.8	13.1	27.7	13.1
Source model (FCOS) [91]	28.4	10.9	53.8	18.9	17.4	13.5	13.2	10.8	20.9	10.7
EPM [32]	30.8	11.5	56.0	16.7	19.6	15.6	16.3	9.9	22.0	11.2
SIGMA [33]	31.5	9.8	59.7	17.5	10.1	14.1	19.3	17.0	22.4	9.5
Oracle	40.5	21.7	67.5	29.5	15.7	37.5	18.5	14.1	30.6	15.7

TABLE 6
Comparison of state-of-the-art unsupervised domain-adaptive object detection methods on Cityscapes→ACDC adaptation for individual conditions. We train a separate model on each condition-specific subset of ACDC and evaluate each model on the condition it has been trained for. Performance of the model trained only on the source domain (Source model) and of oracles with access to the target domain labels for each condition (Oracle) is also reported in AP_{50}^{box}.

Method	Fog	Night	Rain	Snow
Source model [90]	19.7	14.4	23.9	29.2
DA-Faster [28]	17.3	11.6	21.7	29.9
SADA [29]	19.5	17.9	24.0	28.2
MIC (SADA) [30]	24.8	18.4	26.1	31.5
FRCNN-SIGMA++ [31]	23.2	23.2	27.4	33.8
Oracle	28.9	27.9	35.9	41.9
Source model [91]	22.0	14.4	22.6	28.4
EPM [32]	22.3	15.7	21.9	25.8
SIGMA [33]	25.4	18.5	24.4	19.9
Oracle	28.6	28.7	36.2	39.2

importance of realistic adverse-condition images in ACDC. For a fair comparison, we utilize the validation set to pick the best model and report its performance on the test set as described in [33].

From Table 5 we observe that the configuration designed for Cityscapes→Foggy Cityscapes may not be applicable on Cityscapes→ACDC and ACDC demonstrates a challenging benchmark for normal-to-adverse adaptation. Several adversarial-based UDA methods bring losses in performance compared to the source-only model. Other methods presenting limited improvement still have an obvious gap compared to the oracle model. MIC (SADA) exhibits the largest improvement among two-stage object detectors and SIGMA obtains the best performance among one-stage object detectors. Although these models obtain improvement for Cityscapes→Foggy Cityscapes task, the performance drop on Cityscapes→ACDC indicates that the synthetic Foggy Cityscapes is still different from real-world adverse conditions and that ACDC poses a new challenge to existing UDA methods and enables a more realistic setting for domain-adaptive detection.

In addition, we also train state-of-the-art UDA methods to adapt from Cityscapes to individual conditions of ACDC in Table 6. The uniformity of target domain in this setting enables a larger performance gain compared to a target domain with mixed conditions in Table 5. We observe that in some conditions, the UDA method presents even worse performance than the source-only model. This is because the adapted model from the final epoch is not the optimal model for the new domain, which also reflects the importance of hyperparameters on different UDA tasks. Moreover, although the adapted models obtain some performance improvement in a certain condition, the gap between the adapted model and the oracle model is still obvious, indicating the difficulty of ACDC for existing UDA object detection methods.

5 Sensor-Level Adaptation

ACDC also contains 4006 reference images captured in normal conditions, i.e. daytime and clear weather, to which we will refer in the following as ACDC-Reference. As detailed in Sec. 3.3, 1503 of these images have been newly annotated in the present extended version. Thus, we also provide here two new benchmarks for sensor-level adaptation on semantic segmentation and object detection. For this type of adaptation, we use the Cityscapes training set, which is characterized by normal conditions, as the source domain and all ACDC-Reference training images as the target domain. The performance of the adaptation from the camera sensor of Cityscapes to the respective sensor of ACDC is evaluated on the annotated part of the test split of the ACDC-Reference subset, which comprises 500 images.

5.1 Domain-Adaptive Semantic Segmentation

We introduce a new benchmark for sensor-level real-to-real UDA of semantic segmentation: Cityscapes→ACDC-Reference. We select eleven representative state-of-the-art UDA methods, train them with their default configurations for adaptation from Cityscapes to the ACDC-Reference subset and present the results in Table 7. Eight of these methods are trained with the earlier DeepLabv2-based architecture [65], while four of them are trained with the more recent SegFormer-based architecture [88] (CISS [46] is trained with both).

Among the DeepLabv2-based methods, CISS, MRNet and FDA excel on the target-domain test set of ACDC-Reference, as they match (MRNet and FDA) or even exceed (CISS) the

TABLE 7
Comparison of state-of-the-art domain-adaptive semantic segmentation methods on Cityscapes→ACDC-Reference adaptation. Cityscapes serves as the source domain and ACDC-Reference serves as the target domain. The first and second groups of rows present DeepLabv2-based [65] and SegFormer-based [88] unsupervised methods, respectively. The performance of the respective models trained on Cityscapes (Source model) and of the oracle models trained on ACDC-Reference with all its 800 training labels (Oracle) is reported.

Method	road	sidew.	build.	wall	fence	pole	light	sign	veget.	terrain	sky	person	rider	car	truck	bus	train	motorc.	bicycle	mIoU
Source model [65]	84.6	48.2	75.4	26.1	30.5	32.7	30.1	40.0	82.8	56.7	84.2	47.3	45.8	79.2	28.1	45.4	59.0	32.8	52.7	51.7
AdaptSegNet [15]	88.8	58.8	80.6	23.9	33.0	22.9	48.4	39.7	85.8	62.8	94.2	50.6	46.2	61.1	40.5	44.4	53.8	40.5	58.1	54.4
ADVENT [19]	84.9	54.3	83.1	26.3	28.5	23.7	37.5	35.5	85.6	62.7	95.8	53.5	50.2	50.0	48.0	51.4	63.0	43.9	59.2	54.6
BDL [21]	89.4	61.5	80.1	25.4	28.4	22.0	46.8	40.8	85.8	63.3	94.3	48.2	48.7	76.8	43.6	44.3	59.6	46.8	58.9	56.1
CLAN [20]	87.9	49.6	78.5	27.5	29.2	35.9	53.7	49.5	86.3	66.6	90.2	56.0	41.9	80.5	33.4	46.9	61.2	47.7	55.3	56.7
FDA [24]	91.8	66.8	83.3	33.5	33.8	37.6	59.7	55.0	86.4	61.1	93.5	57.3	51.9	81.5	37.4	65.6	61.3	45.4	57.5	61.1
SIM [26]	86.7	50.6	81.4	13.0	28.4	23.9	48.0	35.7	85.5	64.5	91.3	51.0	50.9	72.6	43.0	42.9	53.1	32.8	44.5	52.6
MRNet [27]	90.1	59.4	83.5	31.3	30.1	40.6	59.3	53.7	88.4	67.0	95.6	58.1	55.1	84.4	53.5	44.6	64.8	58.2	64.2	62.2
CISS [46]	92.8	69.2	84.6	34.3	34.4	42.4	59.5	57.4	87.1	61.8	94.7	59.9	54.4	82.7	48.0	66.0	65.7	51.5	61.0	63.5
Oracle	94.1	74.7	86.5	44.3	36.2	39.4	58.3	53.2	87.4	68.8	96.1	56.3	44.7	83.1	42.8	52.5	67.5	45.8	56.7	62.5
Source model [43]	89.1	58.1	89.6	44.1	38.1	54.3	68.6	63.4	91.2	72.6	97.6	66.0	56.5	87.8	50.1	74.7	77.9	55.6	64.0	68.4
DAFormer [43]	92.4	69.9	90.6	63.4	36.5	55.2	70.2	55.9	91.1	70.1	97.6	66.5	57.7	83.5	53.5	74.3	79.7	58.8	62.1	69.9
HRDA [45]	88.8	53.6	92.0	66.4	36.2	58.2	76.6	60.7	91.0	73.0	97.3	76.3	69.1	91.8	70.2	95.0	89.3	68.3	75.3	75.2
MIC [30]	90.9	62.8	92.1	65.5	41.9	61.9	76.7	71.1	88.7	75.0	94.2	76.3	69.5	92.6	72.4	94.7	90.1	70.5	75.6	77.0
CISS [46]	95.8	80.3	92.6	69.0	38.4	60.8	76.9	68.5	92.0	74.3	98.0	76.9	70.6	92.9	71.6	91.9	88.5	69.7	75.5	78.1
Oracle	96.0	80.9	91.3	63.1	45.8	59.0	72.3	66.2	91.6	75.2	98.0	67.8	58.3	86.5	56.3	65.7	80.6	53.6	67.6	72.4

TABLE 8
Comparison of state-of-the-art domain-adaptive object detection methods on Cityscapes→ACDC-Reference adaptation. Cityscapes serves as the source domain and ACDC-Reference serves as the target domain. The first and second groups of rows present two-stage domain-adaptive detection and one-stage domain-adaptive detection methods, respectively. All methods share the same ResNet-50 backbone. The performance of the respective models trained on Cityscapes (Source model) and of the oracle models trained on ACDC-Reference with all its 800 training labels (Oracle) is also reported.

Method	person	rider	car	truck	bus	train	motorc.	bicycle	AP_{50}^{box}	AP^{box}
Source model (Faster R-CNN) [90]	22.1	32.2	45.4	16.4	19.4	20.8	26.7	24.3	25.9	12.6
DA-Faster [28]	21.9	34.8	46.7	13.6	17.5	18.7	26.3	27.6	25.9	12.1
SADA [29]	38.0	40.9	56.3	3.5	6.7	1.7	25.8	29.6	25.3	12.0
MIC (SADA) [30]	35.1	37.9	56.1	8.9	10.5	10.5	29.3	31.4	27.5	12.6
FRCNN-SIGMA++ [31]	21.9	31.2	44.8	18.2	15.8	21.8	27.6	26.9	26.0	12.6
Oracle	24.3	34.6	49.0	31.6	20.5	27.9	34.5	25.0	30.9	15.4
Source model (FCOS) [91]	30.6	28.3	50.6	19.8	21.5	12.6	25.4	21.8	26.3	13.3
EPM [32]	32.3	28.7	52.2	16.8	19.7	12.4	29.2	19.9	26.4	13.4
SIGMA [33]	31.5	31.2	53.6	18.7	17.3	16.9	28.6	26.8	28.1	14.0
Oracle	32.7	56.8	25.5	32.6	29.2	32.6	23.3	24.6	32.2	15.9

mean IoU performance of the oracle model which is trained on labeled images from ACDC-Reference. Thus, we conclude that when focusing on this earlier architecture, the domain gap which is caused by the different sensor characteristics between Cityscapes and ACDC is possible to be closed by state-of-the-art UDA methods. Considering the more recent, SegFormer-based methods, the difference in performance between the source model and the oracle model becomes only slight, namely 4.0% in mean IoU. The three top-performing methods, namely CISS, MIC and HRDA, significantly surpass the performance of the oracle model, indicating that in this domain adaptation setting, the inductive biases which are introduced to the models by the respective aforementioned domain adaptation and generalization strategies boost the target-domain performance even more than the access to in-domain training data, which only the oracle model enjoys.

5.2 Domain-Adaptive Object Detection

We present the sensor-level object detection adaptation results in Table 8. According to the results, although both Cityscapes and ACDC-Reference contain images captured in normal conditions, there still exists a domain gap between Cityscapes and ACDC-Reference. If we take the performance gap between the source-only model and the oracle model as an indicator of the domain gap, Cityscapes has a smaller domain gap to ACDC-Reference set compared to the adverse-condition part of ACDC.

We observe that on common categories such as person and car, state-of-the-art UDA methods for detection obtain equal or better performance compared to the respective oracle models. However, for the less frequent categories such as truck and bus, even if the domain gap is small, there is still an obvious performance gap. This indicates that how to effectively mine the knowledge from these rare categories remains a pressing research question for the area of domain-adaptive object detection.

6 Supervised Learning on Adverse Conditions

In this section, we benchmark several supervised methods for different central dense semantic perception tasks, including semantic

TABLE 9
Comparison of state-of-the-art supervised semantic segmentation methods on ACDC. Training and evaluation are performed using the training and test sets of the entire adverse-condition part of ACDC including all four adverse conditions, respectively.

Method	road	sidew.	build.	wall	fence	pole	light	sign	veget.	terrain	sky	person	rider	car	truck	bus	train	motorc.	bicycle	mIoU
RefineNet [68]	92.5	71.2	86.2	39.0	44.0	53.2	68.8	66.0	85.1	59.3	94.9	65.2	38.5	85.8	53.8	59.7	76.2	47.5	54.5	65.3
DeepLabv2 [65]	88.0	62.3	80.8	37.0	35.1	33.9	49.8	49.5	80.1	50.7	92.5	51.1	26.5	79.9	49.0	41.1	72.2	26.5	44.2	55.3
DeepLabv3+ [74]	93.4	74.8	89.2	53.0	49.0	58.7	71.1	67.4	87.8	62.7	95.9	69.7	36.0	88.1	67.7	71.8	85.1	48.0	59.8	70.0
HRNet [78]	95.3	79.9	90.7	53.7	57.4	65.9	78.4	75.9	88.8	68.6	96.1	75.5	54.0	91.2	68.2	76.2	85.4	58.4	65.1	75.0
Mask2Former [92]	96.2	83.9	91.9	62.0	59.7	70.4	80.4	79.0	90.4	73.0	96.7	78.2	50.8	91.3	74.9	74.3	92.9	57.0	66.1	77.3
ViT-Adapter [93]	96.4	84.6	92.2	68.0	63.7	69.8	80.5	80.0	90.2	72.6	96.4	79.0	48.8	92.0	83.1	68.7	92.3	63.8	68.1	78.4

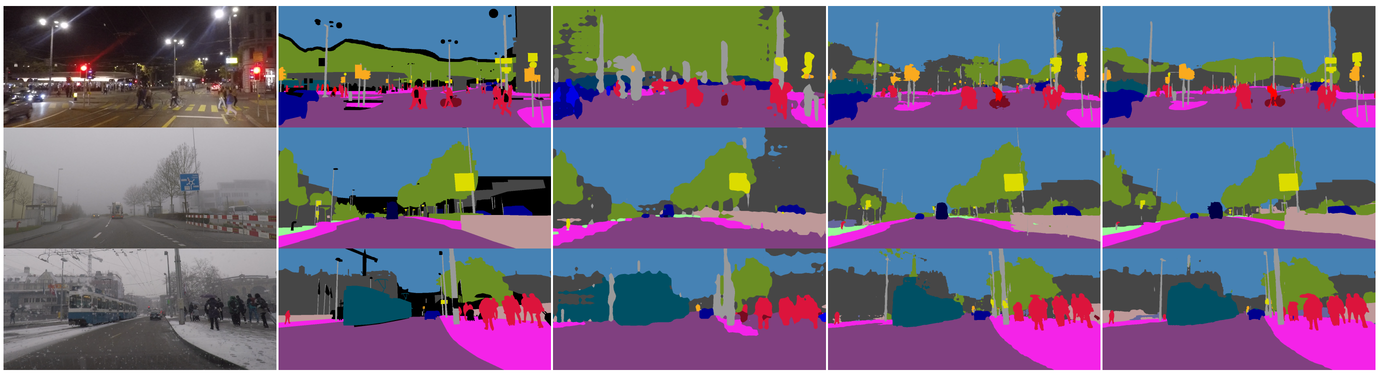

Fig. 4. **Qualitative results of selected semantic segmentation methods on ACDC.** From left to right: image, ground-truth annotation, FDA [24], DeepLabv3+ [74], and HRNet [78]. The color coding of the semantic classes matches Fig. 1.

TABLE 10
Comparison of condition experts vs. uber models on the different conditions of ACDC for semantic segmentation. The first group of rows presents condition-specific expert models trained on a single condition, while the second group presents uber models trained on all adverse conditions. Note that the performance on all conditions is *not* an average of the respective performances on individual conditions.

Method	Fog	Night	Rain	Snow	All
RefineNet [68]	63.6	52.2	66.4	62.5	62.8
DeepLabv2 [65]	52.2	45.4	57.6	56.8	54.9
DeepLabv3+ [74]	68.7	59.2	73.5	70.5	69.6
HRNet [78]	70.8	63.2	72.7	70.2	70.9
RefineNet [68]	65.7	55.5	68.7	65.9	65.3
DeepLabv2 [65]	54.5	45.3	59.3	57.1	55.3
DeepLabv3+ [74]	69.1	60.9	74.1	69.6	70.0
HRNet [78]	74.7	65.3	77.7	76.3	75.0

segmentation, instance segmentation, and panoptic segmentation, on ACDC.

6.1 Semantic Segmentation

We use ACDC to train six state-of-the-art supervised semantic segmentation methods and report their performance in Table 9. Qualitative results are shown in Fig. 4 for two supervised methods and one UDA method. We draw the following conclusions: (1) full supervision in adverse conditions is more valuable than designing a better architecture trained solely on normal conditions, as even an earlier method [65] performs better with full supervision than the top-performing externally pre-trained model (cf. Table 17). (2) ACDC is a challenging benchmark for supervised methods due to its hard visual domains; even the very recent ViT-Adapter [93] scores only 78.4% mIoU on the test set, which is 6.8% lower than its respective performance of 85.2% on Cityscapes [78]. (3) The rankings of the supervised and the pre-trained models do not correlate well, as can be seen from the results in Tables 9 and 17.

The last point suggests that state-of-the-art networks such as HRNet have enough capacity to overfit to datasets such as Cityscapes, which would explain the low performance of the Cityscapes pre-trained HRNet model on ACDC. We test this hypothesis by training HRNet *jointly on Cityscapes and ACDC*; our expectation is that the jointly trained model will at least match the performance of the individually trained models on each dataset. This is confirmed, as the jointly trained model gets 81.2% mIoU on Cityscapes and 74.8% on ACDC, beating and being on a par with the respective individually trained models. Thus, even if ACDC is not of very large scale, it helps to efficiently regularize segmentation models for normal conditions as well.

Table 10 compares models trained on a single adverse condition, termed condition experts, against models trained on the entire training set, termed uber models. Each condition expert is evaluated on the condition it has been trained on. The uber models generally beat the respective condition experts across different conditions and segmentation networks. This hints that the capacity of these networks is large enough to discover discriminative representations for all conditions simultaneously. We also evaluate ensembles of condition experts against uber models on the complete test set ("All"), where the ensemble uses the expert corresponding to the condition of the input image for prediction. Again, the uber models outperform the ensembles of experts for all examined methods. Moreover, all methods perform worst at nighttime, indicating that the nighttime set of ACDC represents a

TABLE 11
Comparison of class-level performance of DeepLabv3+ condition experts on the various conditions of ACDC. A different model is trained on each individual condition and then evaluated on this condition.

Condition	road	sidew.	build.	wall	fence	pole	light	sign	veget.	terrain	sky	person	rider	car	truck	bus	train	motorc.	bicycle	mIoU
Fog	93.8	77.4	88.8	51.0	43.3	54.2	68.2	71.7	87.7	74.6	98.2	53.5	32.1	83.8	69.3	84.4	85.3	47.2	40.1	68.7
Night	94.7	75.9	85.0	48.4	38.6	52.2	55.8	54.4	76.1	30.3	84.2	67.4	41.1	85.0	8.3	62.3	80.6	35.6	49.8	59.2
Rain	92.8	77.4	93.9	67.3	58.1	64.1	74.4	75.9	94.2	50.8	98.6	70.8	33.4	90.4	67.7	79.2	86.8	54.6	66.1	73.5
Snow	91.9	70.9	90.1	48.9	52.0	62.2	79.2	74.5	92.0	47.0	97.6	78.2	35.9	90.4	61.7	64.3	89.2	43.9	69.4	70.5

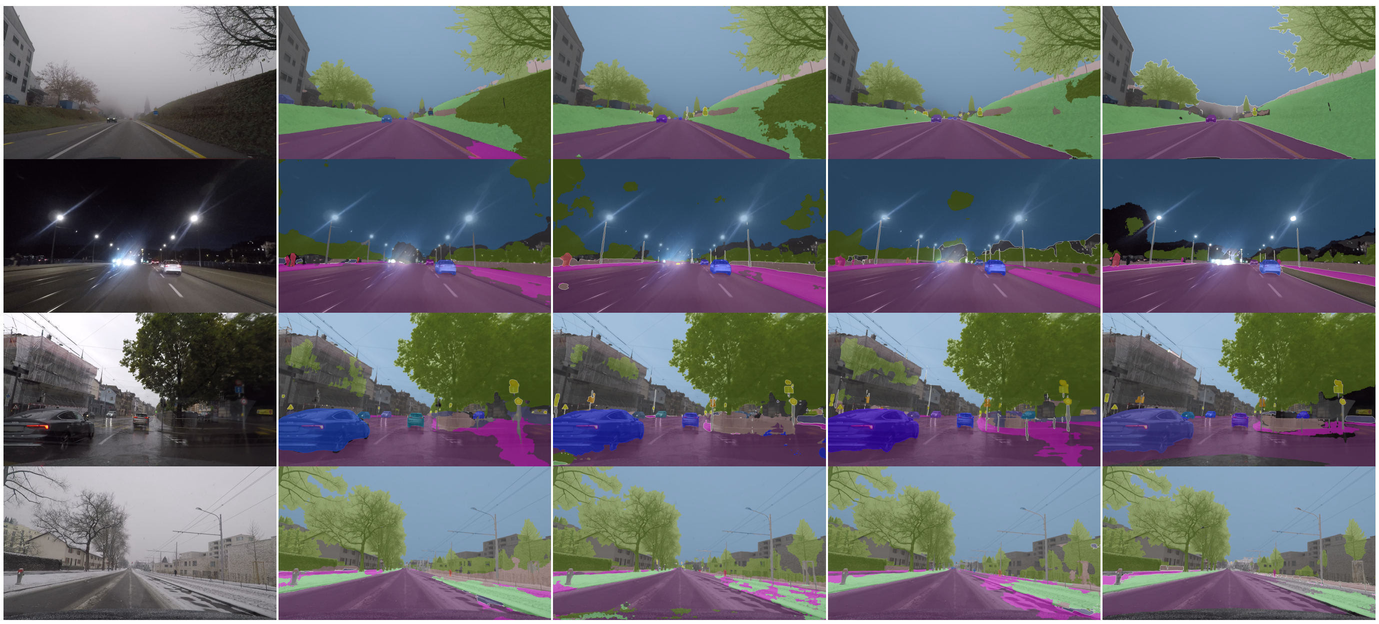

Fig. 5. **Qualitative results of panoptic segmentation methods on ACDC.** From left to right: image, Panoptic FPN [94], K-Net [95], Panoptic-Deeplab [96], and Mask2Former [92]. The color coding of the semantic classes matches Fig. 1.

TABLE 12
Cross-evaluation of DeepLabv3+ condition experts on the various adverse conditions of ACDC. Each model is trained on an individual condition and evaluated on each condition separately. Performance of the Cityscapes pre-trained model is also reported.

Train/Eval	Fog	Night	Rain	Snow
Normal	45.7	25.0	50.0	42.0
Fog	68.7	40.7	63.5	59.1
Night	58.5	59.2	55.6	49.6
Rain	65.2	46.0	73.5	63.5
Snow	59.2	38.0	69.3	70.5

harder domain than the other sets.

We focus on the widely used DeepLabv3+ network [74] for a detailed study of class-level performance across different conditions and compare the performance of the four condition experts in Table 11. We make the following observations: (1) the lowest performance for *road* and *sidewalk* occurs in snow, which can be attributed to confusion between the two classes due to similar appearance in the presence of snow cover. (2) Classes that usually appear dark or are not well-lit at nighttime, e.g., *building*, *vegetation*, *traffic sign*, and *sky*, are harder to segment at nighttime. (3) Performance on classes with instances of small size, such as *person*, *rider*, and *bicycle*, is lowest on fog, probably due to the combined effect of contrast reduction and low resolution for instances of these classes that are far from the camera.

We also evaluate in Table 12 the four DeepLabv3+ condition experts on conditions that are not encountered at training. Excluding nighttime, the results are close to symmetric with respect to training versus evaluation condition; e.g., training on fog and testing on snow results in a similar performance to training on snow and testing on fog. In contrast, performance of the night expert on other conditions is much higher than performance of other experts at night, implying that representations learned from the nighttime domain can generalize better to the other adverse conditions than vice versa.

6.2 Instance Segmentation

We use ACDC to train four popular supervised instance segmentation methods and report their performance in Table 13. Detectors obtain the best performance in object detection with 26.6% AP^{box} and instance segmentation with 23.5% AP^{mask} simultaneously. Although HTC presents better AP^{box}_{50} and AP^{mask}_{50} than Detectors, Detectors exhibit a better capability of localization and achieve better performance at higher IoU thresholds, namely on AP^{box}_{75} and AP^{mask}_{75}.

In Table 14, we compare the instance segmentation performance of condition experts versus uber models, similarly to Ta-

TABLE 13
Comparison of state-of-the-art supervised instance segmentation methods on ACDC. Training and evaluation are performed using the training and test sets of the entire adverse-condition part of ACDC including all four adverse conditions, respectively.

Method	AP^{box}	AP^{box}_{50}	AP^{box}_{75}	AP^{mask}	AP^{mask}_{50}	AP^{mask}_{75}
Mask R-CNN [86]	22.7	43.4	20.9	20.7	39.7	19.0
Cascaded Mask R-CNN [97]	24.4	42.1	24.1	21.3	39.5	20.4
HTC [98]	26.0	45.2	26.0	23.0	41.9	22.0
Detectors [99]	26.6	44.3	27.0	23.5	41.8	22.3

TABLE 14
Comparison of condition experts vs. uber models on the different conditions of ACDC for instance segmentation. The first group of rows presents condition-specific expert models trained on a single condition, while the second group presents uber models trained on all adverse conditions. For each condition we report the performance in AP^{mask} separately. Note that the performance on all conditions is *not* an average of the respective performances on individual conditions.

Method	Fog	Night	Rain	Snow	All
Mask R-CNN [86]	15.6	10.7	21.3	20.8	16.8
Cascaded MRCNN [97]	16.2	11.5	21.2	22.3	17.9
HTC [98]	17.3	12.4	22.3	23.4	18.8
Detectors [99]	17.4	13.1	23.3	23.4	19.0
Mask R-CNN [86]	24.4	14.2	21.6	27.4	20.7
Cascaded MRCNN [97]	24.3	13.9	22.5	28.2	21.3
HTC [98]	26.0	15.4	23.2	30.2	23.0
Detectors [99]	25.3	16.5	24.9	29.8	23.5

ble 10. Generally, across different instance segmentation architectures, uber models outperform condition experts, which are only optimized on a single condition. Night is still the most challenging condition for all methods. We also observe that the performance gap between the uber model and the condition expert model is the highest in fog, which indicates that images exhibiting different appearance shifts from the one induced by fog can still benefit a model's robustness to fog a lot, even though such images are characterized by a significant domain gap to the target condition of fog.

6.3 Panoptic Segmentation

We use ACDC to train four popular supervised panoptic segmentation methods and report their performance in Table 15. Qualitative results are shown in Fig. 5. Mask2Former obtains the best PQ and PQ^{stuff} performance among these methods, while a simple PanopticFPN obtains the best PQ^{things}. We also present a comparison between condition experts and uber models for panoptic segmentation in Table 16. Mask2Former exhibits advantages in most conditions. At the same time, uber models outperform most condition experts by a large margin. Interestingly, we observe that unlike supervised semantic segmentation and instance segmentation, in rain, the uber models are roughly on a par with the rain experts across the four examined architectures. This indicates that the domain shifts in other conditions with respect to rain provide limited help in distinguishing the categories in rain.

TABLE 15
Comparison of state-of-the-art supervised panoptic segmentation methods on ACDC. Training and evaluation are performed using the training and test sets of the entire adverse-condition part of ACDC including all four adverse conditions, respectively.

Method	PQ	PQ^{things}	PQ^{stuff}	SQ	RQ
PanopticFPN [94]	43.9	36.4	49.3	77.6	54.6
K-Net [95]	47.2	30.5	59.4	77.8	58.8
Panoptic-Deeplab [96]	49.4	35.5	59.5	79.7	60.1
Mask2Former [92]	49.8	33.9	61.3	80.0	60.7

TABLE 16
Comparison of condition experts vs. uber models on the different conditions of ACDC for panoptic segmentation. The first group of rows presents condition-specific expert models trained on a single condition, while the second group presents uber models trained on all adverse conditions. For each case we report the performance in PQ. Note that the performance on all conditions is *not* an average of the respective performances on individual conditions.

Method	Fog	Night	Rain	Snow	All
PanopticFPN [94]	38.4	29.8	46.7	44.8	41.3
K-Net [95]	37.9	30.7	48.5	48.0	43.3
Panoptic-Deeplab [96]	42.4	34.1	52.7	51.6	46.7
Mask2Former [92]	44.9	34.0	53.0	52.5	47.1
PanopticFPN [94]	43.9	32.6	43.9	49.1	44.3
K-Net [95]	47.8	33.4	47.1	53.2	45.6
Panoptic-Deeplab [96]	49.1	37.2	53.1	55.1	49.4
Mask2Former [92]	52.9	39.4	54.2	58.6	51.1

7 Evaluation of Externally Pre-trained Models

In this section, we evaluate on ACDC models that have been pre-trained on external datasets, for various semantic perception tasks.

7.1 Semantic Segmentation

In Table 17, we use ACDC to evaluate semantic segmentation models which have been pre-trained on external datasets. For models pre-trained on Cityscapes, the performance drop is larger on the nighttime set, implying that the domain shift from the normal-condition domain is larger for this set. Methods that specialize on fog or nighttime generally perform better on that condition compared to models pre-trained on Cityscapes. Moreover, most of these specialized methods also improve the performance on conditions other than the one encountered at training time.

7.2 Instance Segmentation

In Table 18, we evaluate various models pre-trained on Cityscapes for instance segmentation. All these instance segmentation models

TABLE 17
Comparison of externally pre-trained semantic segmentation models on ACDC for individual conditions and jointly for all adverse conditions. The three groups of rows present models pre-trained on normal, foggy, and nighttime conditions respectively. CS: Cityscapes [1], FC: Foggy Cityscapes [36], FC-DBF: Foggy Cityscapes-DBF [38], FZ: Foggy Zurich [38], ND: Nighttime Driving [39], DZ: Dark Zurich [9].

Method	Trained on	Fog	Night	Rain	Snow	All
RefineNet [68]	CS	46.4	29.0	52.6	43.3	43.7
DeepLabv2 [65]	CS	33.5	30.1	44.5	40.2	38.0
DeepLabv3+ [74]	CS	45.7	25.0	50.0	42.0	41.6
DANet [76]	CS	34.7	19.1	41.5	33.3	33.1
HRNet [78]	CS	38.4	20.6	44.8	35.1	35.3
SFSU [36]	FC	45.6	29.5	51.6	41.4	42.9
CMAda [38]	FC-DBF+FZ	51.2	32.0	53.4	47.6	47.1
DMAda [39]	ND	50.7	32.7	54.9	48.9	47.9
GCMA [40]	CS+DZ	52.4	42.9	58.0	53.8	53.4
MGCDA [9]	CS+DZ	45.9	40.8	54.2	50.5	48.9
DANNet [100]	CS+DZ	–	47.6	–	–	–

TABLE 18
Comparison of externally pre-trained instance segmentation models on ACDC for individual conditions and jointly for all adverse conditions. The two groups of rows present performance in AP^{box} and AP^{mask} respectively. CS: Cityscapes [1].

Method	Trained on	Fog	Night	Rain	Snow	All
Mask R-CNN [86]	CS	11.1	4.8	12.8	14.3	10.2
Cascaded Mask R-CNN [97]	CS	11.1	5.3	13.3	15.5	10.6
HTC [98]	CS	7.6	2.6	9.2	9.2	6.5
Detectors [99]	CS	12.1	3.8	12.9	12.7	9.4
Mask R-CNN [86]	CS	9.8	3.6	11.0	12.9	8.8
Cascaded Mask R-CNN [97]	CS	9.8	3.9	11.8	12.5	9.0
HTC [98]	CS	7.0	2.3	8.4	8.3	5.9
Detectors [99]	CS	10.1	2.6	10.9	10.1	7.8

exhibit rather low performance on ACDC, indicating that there is a large domain gap between Cityscapes and ACDC. Night is the most challenging condition for all these pre-trained models. Although HTC brings improvement in the supervised setting compared to Mask R-CNN and Cascaded Mask R-CNN as we have discussed in Table 13, it deteriorates the out-of-distribution performance in the present case of external pre-training. As HTC enhances the correlation of mask branches in different stages with interleaved execution, apparently the domain-specific bias is also strengthened and a worse out-of-distribution robustness is thus induced. As Detectors are built on top of HTC, they also exhibit a limited out-of-distribution performance on ACDC.

7.3 Panoptic Segmentation

In Table 19, we report the performance of Cityscapes-pre-trained panoptic segmentation models on ACDC adverse-condition images. We also observe a performance drop caused by the domain shift between Cityscapes and ACDC on state-of-the-art panoptic segmentation models. Moreover, the transformer-based Mask2Former outperforms the convolutional methods PanopticFPN and Panoptic-Deeplab. Interestingly, we also find that both mask-based methods, including K-Net and Mask2Former, present a substantially better generalization ability than per-pixel classification based methods. This indicates the mask-based methods are less affected by the domain shift in adverse conditions. However, even though the transformer-based Mask2Former model pre-trained on normal conditions shows impressive robustness to adverse conditions, it still performs much worse than the Mask2Former model which has been specifically trained on adverse conditions. By introducing the panoptically annotated extension of our ACDC dataset, we hope that the latter will contribute to closing this performance gap by fostering the development of both normal-to-adverse panoptic segmentation adaptation methods and more robust and generalizable supervised panoptic segmentation methods.

TABLE 19
Comparison of externally pre-trained panoptic segmentation models on ACDC for individual conditions and jointly for all adverse conditions. We report the performance in PQ for different conditions. CS: Cityscapes [1].

Method	Trained on	Fog	Night	Rain	Snow	All
PanopticFPN [94]	CS	15.9	4.0	18.6	13.1	13.0
K-Net [95]	CS	17.3	6.0	23.0	18.7	16.7
Panoptic-Deeplab [96]	CS	6.5	1.6	8.3	1.6	4.7
Mask2Former [92]	CS	42.7	19.9	41.4	42.0	37.7

TABLE 20
Uncertainty-aware semantic segmentation baseline results using AUIoU. Supervised methods for standard semantic segmentation are trained and evaluated either separately on each condition or jointly on all adverse conditions for semantic label prediction. Confidence prediction baselines: globally constant and equal to 100% (Constant 100%), max-softmax network outputs (Max-Softmax), ground-truth invalid masks (GT).

Method	Confidence	Fog	Night	Rain	Snow	All
RefineNet [68]	Constant 100%	63.6	52.2	66.4	62.5	65.3
RefineNet [68]	Max-Softmax	60.6	51.4	62.5	59.9	62.5
RefineNet [68]	GT	67.9	61.1	67.9	64.0	68.8
DeepLabv2 [65]	Constant 100%	52.2	45.4	57.6	56.8	55.3
DeepLabv2 [65]	Max-Softmax	51.9	45.9	56.0	56.8	54.7
DeepLabv2 [65]	GT	56.7	54.7	59.1	58.4	58.9
DeepLabv3+ [74]	Constant 100%	68.7	59.2	73.5	70.5	70.0
DeepLabv3+ [74]	Max-Softmax	66.4	59.1	70.6	67.9	67.8
DeepLabv3+ [74]	GT	73.1	67.1	75.0	72.0	73.3

8 Uncertainty-Aware Semantic Segmentation

Existing works that model uncertainty in semantic segmentation [101], [102] are evaluated only with IoU, which does not assess the predicted confidence. In contrast, for uncertainty-aware semantic segmentation, algorithms are required to output both a hard semantic prediction $\hat{H}$ and a confidence map C with values in the range $[0, 1]$. The average UIoU (AUIoU) metric is computed by thresholding C at multiple thresholds across the range $[0, 1]$, calculating the UIoU [9] for each threshold and averaging the results. A pixel p with confidence value below the examined threshold is treated as invalid and contributes positively if $J(p) = 1$ (true invalid) and negatively if $J(p) = 0$ (false invalid).

8.1 Baselines and Oracles

We present the results of straightforward baselines for uncertainty-aware semantic segmentation that are based on methods for standard semantic segmentation in Table 20. We first evaluate three state-of-the-art methods using confidence maps that are constant and equal to 1, i.e., not modeling confidence. In this case, AUIoU reduces to IoU. Any sensible method that models confidence should improve upon this baseline. Using the max-softmax scores output by these methods as confidence maps generally yields inferior results to globally constant confidence, as softmax is not a good proxy for confidence. An upper bound for the performance of the examined methods is obtained by using a confidence oracle. More specifically, we use the binary complement of the ground-truth invalid mask J as the confidence prediction. This raises AUIoU performance significantly across all conditions compared to the globally constant confidence baseline. The performance gap between the oracle and the baseline is largest for night, indicating that explicitly modeling uncertainty has the potential to improve performance especially in the nighttime domain.

We have also trained [101] on ACDC, using the GT invalid masks for training its outlier detection part. The learned confidence by [101] leads to lower test set AUIoU (52.0%) than constant confidence (53.0%), indicating that a better modeling of uncertainty is needed in future approaches.

9 Conclusion

In this paper, we have presented ACDC, a large-scale dataset and benchmark suite for robust semantic driving scene perception. Our dataset covers adverse visual domains that are common in driving scenarios and features high-quality pixel-level panoptic annotations which also include visually degraded image regions, while the present extended version also includes normal-condition annotations, completing the condition span of the dataset. Our annotations support a wide range of five dense semantic perception tasks: standard and uncertainty-aware semantic segmentation, object detection, instance segmentation, and panoptic segmentation.

We have evaluated several state-of-the-art approaches on our benchmark, both in the supervised and the unsupervised setting. The conclusions from this evaluation show the importance of ACDC in steering future progress in the field: (i) ACDC provides a challenging, real-world target domain for unsupervised domain adaptation approaches to various semantic perception tasks both in the normal-to-adverse adaptation setting and in the sensor-level adaptation setting, (ii) ACDC is a hard benchmark for supervised semantic perception, as state-of-the-art methods generally score much lower on it than on standard normal-condition benchmarks such as Cityscapes, (iii) ACDC can be used jointly with existing normal-condition datasets for training in order to regularize models better and improve their performance both under normal and adverse conditions.

Acknowledgments

This work is funded by Toyota Motor Europe via the research project TRACE-Zürich. We thank Anton Obukhov and Yuhang Lu for their advice on running HRNet and DANet.

References

[1] M. Cordts, M. Omran, S. Ramos, T. Rehfeld, M. Enzweiler, R. Benenson, U. Franke, S. Roth, and B. Schiele, "The Cityscapes dataset for semantic urban scene understanding," in *The IEEE Conference on Computer Vision and Pattern Recognition (CVPR)*, 2016. 1, 2, 3, 4, 5, 13

[2] G. Neuhold, T. Ollmann, S. Rota Bulò, and P. Kontschieder, "The Mapillary Vistas dataset for semantic understanding of street scenes," in *The IEEE International Conference on Computer Vision (ICCV)*, 2017. 1, 3, 5

[3] A. Geiger, P. Lenz, and R. Urtasun, "Are we ready for autonomous driving? The KITTI vision benchmark suite," in *IEEE Conference on Computer Vision and Pattern Recognition (CVPR)*, 2012. 1, 3

[4] W. Maddern, G. Pascoe, C. Linegar, and P. Newman, "1 year, 1000 km: The Oxford RobotCar dataset," *The International Journal of Robotics Research*, vol. 36, no. 1, pp. 3–15, 2017. 1, 3

[5] F. Yu, H. Chen, X. Wang, W. Xian, Y. Chen, F. Liu, V. Madhavan, and T. Darrell, "BDD100K: A diverse driving dataset for heterogeneous multitask learning," in *IEEE/CVF Conference on Computer Vision and Pattern Recognition (CVPR)*, June 2020. 1, 3, 5, 6

[6] P. Wenzel, R. Wang, N. Yang, Q. Cheng, Q. Khan, L. von Stumberg, N. Zeller, and D. Cremers, "4Seasons: A cross-season dataset for multi-weather SLAM in autonomous driving," in *Proceedings of the German Conference on Pattern Recognition (GCPR)*, 2020. 1

[7] P. Sun, H. Kretzschmar, X. Dotiwalla, A. Chouard, V. Patnaik, P. Tsui, J. Guo, Y. Zhou, Y. Chai, B. Caine, V. Vasudevan, W. Han, J. Ngiam, H. Zhao, A. Timofeev, S. Ettinger, M. Krivokon, A. Gao, A. Joshi, Y. Zhang, J. Shlens, Z. Chen, and D. Anguelov, "Scalability in perception for autonomous driving: Waymo open dataset," in *IEEE/CVF Conference on Computer Vision and Pattern Recognition (CVPR)*, June 2020. 1, 3

[8] H. Caesar, V. Bankiti, A. H. Lang, S. Vora, V. E. Liong, Q. Xu, A. Krishnan, Y. Pan, G. Baldan, and O. Beijbom, "nuScenes: A multimodal dataset for autonomous driving," in *IEEE/CVF Conference on Computer Vision and Pattern Recognition (CVPR)*, June 2020. 1, 3

[9] C. Sakaridis, D. Dai, and L. Van Gool, "Map-guided curriculum domain adaptation and uncertainty-aware evaluation for semantic nighttime image segmentation," *IEEE Transactions on Pattern Analysis and Machine Intelligence*, 2020. 1, 2, 3, 6, 7, 13

[10] O. Zendel, K. Honauer, M. Murschitz, D. Steininger, and G. Fernandez Dominguez, "WildDash - creating hazard-aware benchmarks," in *The European Conference on Computer Vision (ECCV)*, 2018. 1, 3, 6

[11] Y. Zhang, P. David, and B. Gong, "Curriculum domain adaptation for semantic segmentation of urban scenes," in *The IEEE International Conference on Computer Vision (ICCV)*, 2017. 2

[12] J. Hoffman, E. Tzeng, T. Park, J.-Y. Zhu, P. Isola, K. Saenko, A. Efros, and T. Darrell, "CyCADA: Cycle-consistent adversarial domain adaptation," in *International Conference on Machine Learning*, 2018. 2, 3

[13] S. Sankaranarayanan, Y. Balaji, A. Jain, S. Nam Lim, and R. Chellappa, "Learning from synthetic data: Addressing domain shift for semantic segmentation," in *IEEE Conference on Computer Vision and Pattern Recognition (CVPR)*, June 2018. 2, 3

[14] Y. Zhang, Z. Qiu, T. Yao, D. Liu, and T. Mei, "Fully convolutional adaptation networks for semantic segmentation," in *The IEEE Conference on Computer Vision and Pattern Recognition (CVPR)*, 2018. 2, 3

[15] Y.-H. Tsai, W.-C. Hung, S. Schulter, K. Sohn, M.-H. Yang, and M. Chandraker, "Learning to adapt structured output space for semantic segmentation," in *The IEEE Conference on Computer Vision and Pattern Recognition (CVPR)*, 2018. 2, 3, 7, 9

[16] Y. Chen, W. Li, and L. Van Gool, "ROAD: Reality oriented adaptation for semantic segmentation of urban scenes," in *The IEEE Conference on Computer Vision and Pattern Recognition (CVPR)*, 2018. 2, 3

[17] Z. Wu, X. Han, Y.-L. Lin, M. G. Uzunbas, T. Goldstein, S. Nam Lim, and L. S. Davis, "DCAN: Dual channel-wise alignment networks for unsupervised scene adaptation," in *The European Conference on Computer Vision (ECCV)*, 2018. 2

[18] Y. Zou, Z. Yu, B. Vijaya Kumar, and J. Wang, "Unsupervised domain adaptation for semantic segmentation via class-balanced self-training," in *The European Conference on Computer Vision (ECCV)*, 2018. 2, 3

[19] T.-H. Vu, H. Jain, M. Bucher, M. Cord, and P. Perez, "ADVENT: Adversarial entropy minimization for domain adaptation in semantic segmentation," in *The IEEE Conference on Computer Vision and Pattern Recognition (CVPR)*, 2019. 2, 3, 7, 9

[20] Y. Luo, L. Zheng, T. Guan, J. Yu, and Y. Yang, "Taking a closer look at domain shift: Category-level adversaries for semantics consistent

domain adaptation," in *The IEEE Conference on Computer Vision and Pattern Recognition (CVPR)*, 2019. 2, 3, 7, 9

[21] Y. Li, L. Yuan, and N. Vasconcelos, "Bidirectional learning for domain adaptation of semantic segmentation," in *The IEEE Conference on Computer Vision and Pattern Recognition (CVPR)*, 2019. 2, 3, 7, 9

[22] Y.-H. Tsai, K. Sohn, S. Schulter, and M. Chandraker, "Domain adaptation for structured output via discriminative patch representations," in *IEEE/CVF International Conference on Computer Vision (ICCV)*, October 2019. 2, 3

[23] Y. Zou, Z. Yu, X. Liu, B. V. Kumar, and J. Wang, "Confidence regularized self-training," in *IEEE/CVF International Conference on Computer Vision (ICCV)*, October 2019. 2, 3, 7

[24] Y. Yang and S. Soatto, "FDA: Fourier domain adaptation for semantic segmentation," in *IEEE/CVF Conference on Computer Vision and Pattern Recognition (CVPR)*, June 2020. 2, 3, 7, 9, 10

[25] M. Kim and H. Byun, "Learning texture invariant representation for domain adaptation of semantic segmentation," in *IEEE/CVF Conference on Computer Vision and Pattern Recognition (CVPR)*, June 2020. 2, 3

[26] Z. Wang, M. Yu, Y. Wei, R. Feris, J. Xiong, W.-m. Hwu, T. S. Huang, and H. Shi, "Differential treatment for stuff and things: A simple unsupervised domain adaptation method for semantic segmentation," in *IEEE/CVF Conference on Computer Vision and Pattern Recognition (CVPR)*, June 2020. 2, 3, 7, 9

[27] Z. Zheng and Y. Yang, "Rectifying pseudo label learning via uncertainty estimation for domain adaptive semantic segmentation," *International Journal of Computer Vision*, 2021. 2, 7, 9

[28] Y. Chen, W. Li, C. Sakaridis, D. Dai, and L. Van Gool, "Domain adaptive faster r-cnn for object detection in the wild," in *IEEE Conference on Computer Vision and Pattern Recognition (CVPR)*, 2018. 2, 8, 9

[29] Y. Chen, H. Wang, W. Li, C. Sakaridis, D. Dai, and L. Van Gool, "Scale-aware domain adaptive faster r-cnn," *IJCV*, vol. 129, no. 7, pp. 2223–2243, 2021. 2, 8, 9

[30] L. Hoyer, D. Dai, H. Wang, and L. Van Gool, "MIC: Masked image consistency for context-enhanced domain adaptation," in *Proceedings of the IEEE/CVF Conference on Computer Vision and Pattern Recognition (CVPR)*, 2023. 2, 3, 7, 8, 9

[31] W. Li, X. Liu, and Y. Yuan, "Sigma++: Improved semantic-complete graph matching for domain adaptive object detection," *IEEE Transactions on Pattern Analysis and Machine Intelligence*, pp. 1–18, 2023. 2, 8, 9

[32] H. Cheng-Chun, T. Yi-Hsuan, L. Yen-Yu, and M.-H. Yang, "Every pixel matters: Center-aware feature alignment for domain adaptive object detector," in *European Conference on Computer Vision*, 2020. 2, 8, 9

[33] W. Li, X. Liu, and Y. Yuan, "Sigma: Semantic-complete graph matching for domain adaptive object detection," in *CVPR*, 2022. 2, 8, 9

[34] S. R. Richter, V. Vineet, S. Roth, and V. Koltun, "Playing for data: Ground truth from computer games," in *European Conference on Computer Vision*. Springer, 2016. 2, 3

[35] G. Ros, L. Sellart, J. Materzynska, D. Vazquez, and A. M. Lopez, "The SYNTHIA dataset: A large collection of synthetic images for semantic segmentation of urban scenes," in *The IEEE Conference on Computer Vision and Pattern Recognition (CVPR)*, June 2016. 2, 3

[36] C. Sakaridis, D. Dai, and L. Van Gool, "Semantic foggy scene understanding with synthetic data," *International Journal of Computer Vision*, vol. 126, no. 9, pp. 973–992, 2018. 2, 3, 6, 13

[37] ——, "ACDC: The Adverse Conditions Dataset with Correspondences for semantic driving scene understanding," in *Proceedings of the IEEE/CVF International Conference on Computer Vision (ICCV)*, 2021. 2, 3

[38] C. Sakaridis, D. Dai, S. Hecker, and L. Van Gool, "Model adaptation with synthetic and real data for semantic dense foggy scene understanding," in *The European Conference on Computer Vision (ECCV)*, 2018. 2, 3, 13

[39] D. Dai and L. Van Gool, "Dark model adaptation: Semantic image segmentation from daytime to nighttime," in *IEEE International Conference on Intelligent Transportation Systems*, 2018. 2, 3, 6, 13

[40] C. Sakaridis, D. Dai, and L. Van Gool, "Guided curriculum model adaptation and uncertainty-aware evaluation for semantic nighttime image segmentation," in *The IEEE International Conference on Computer Vision (ICCV)*, 2019. 2, 13

[41] S. Di, Q. Feng, C.-G. Li, M. Zhang, H. Zhang, S. Elezovikj, C. C. Tan, and H. Ling, "Rainy night scene understanding with near scene semantic adaptation," *IEEE Transactions on Intelligent Transportation Systems*, vol. 22, no. 3, pp. 1594–1602, 2021. 2

[42] H. Porav, T. Bruls, and P. Newman, "Don't worry about the weather: Unsupervised condition-dependent domain adaptation," in *2019 IEEE Intelligent Transportation Systems Conference (ITSC)*, 2019, pp. 33–40. 2

[43] L. Hoyer, D. Dai, and L. Van Gool, "DAFormer: Improving network architectures and training strategies for domain-adaptive semantic segmentation," in *Proceedings of the IEEE/CVF Conference on Computer Vision and Pattern Recognition (CVPR)*, 2022. 2, 3, 7, 9

[44] B. Xie, S. Li, M. Li, C. H. Liu, G. Huang, and G. Wang, "SePiCo: Semantic-guided pixel contrast for domain adaptive semantic segmentation," *IEEE Transactions on Pattern Analysis and Machine Intelligence*, vol. 45, no. 7, pp. 9004–9021, 2023. 2, 3, 7

[45] L. Hoyer, D. Dai, and L. Van Gool, "HRDA: Context-aware high-resolution domain-adaptive semantic segmentation," in *The European Conference on Computer Vision (ECCV)*, 2022. 2, 3, 7, 9

[46] C. Sakaridis, D. Bruggemann, F. Yu, and L. Van Gool, "Condition-invariant semantic segmentation," *arXiv preprint arXiv:2305.17349*, 2023. 2, 3, 7, 8, 9

[47] D. Bruggemann, C. Sakaridis, P. Truong, and L. Van Gool, "Refign: Align and refine for adaptation of semantic segmentation to adverse conditions," in *Proceedings of the IEEE/CVF Winter Conference on Applications of Computer Vision (WACV)*, 2023. 2, 3

[48] D. Bruggemann, C. Sakaridis, T. Broedermann, and L. Van Gool, "Contrastive model adaptation for cross-condition robustness in semantic segmentation," in *Proceedings of the IEEE/CVF International Conference on Computer Vision (ICCV)*, 2023. 2, 3

[49] X. Huang, P. Wang, X. Cheng, D. Zhou, Q. Geng, and R. Yang, "The ApolloScape open dataset for autonomous driving and its application," *IEEE Transactions on Pattern Analysis and Machine Intelligence*, vol. 42, no. 10, pp. 2702–2719, 2020. 3

[50] S. R. Richter, Z. Hayder, and V. Koltun, "Playing for benchmarks," in *Proceedings of the IEEE International Conference on Computer Vision (ICCV)*, October 2017. 3

[51] M. Johnson-Roberson, C. Barto, R. Mehta, S. N. Sridhar, K. Rosaen, and R. Vasudevan, "Driving in the matrix: Can virtual worlds replace human-generated annotations for real world tasks?" in *IEEE International Conference on Robotics and Automation*, 2017. 3

[52] T. Sun, M. Segu, J. Postels, Y. Wang, L. Van Gool, B. Schiele, F. Tombari, and F. Yu, "SHIFT: A synthetic driving dataset for continuous multi-task domain adaptation," in *Proceedings of the IEEE/CVF Conference on Computer Vision and Pattern Recognition (CVPR)*, 2022. 3

[53] S. S. Halder, J.-F. Lalonde, and R. de Charette, "Physics-based rendering for improving robustness to rain," in *Proceedings of the IEEE/CVF International Conference on Computer Vision (ICCV)*, October 2019. 3

[54] M. Bijelic, T. Gruber, F. Mannan, F. Kraus, W. Ritter, K. Dietmayer, and F. Heide, "Seeing through fog without seeing fog: Deep multimodal sensor fusion in unseen adverse weather," in *Proceedings of the IEEE/CVF Conference on Computer Vision and Pattern Recognition (CVPR)*, June 2020. 3

[55] M. Pitropov, D. E. Garcia, J. Rebello, M. Smart, C. Wang, K. Czarnecki, and S. Waslander, "Canadian adverse driving conditions dataset," *The International Journal of Robotics Research*, 2020. 3

[56] B. Zhou, P. Krähenbühl, and V. Koltun, "Does computer vision matter for action?" *Science Robotics*, vol. 4, no. 30, 2019. 3

[57] A. Pfeuffer, M. Schön, D. Carsten, and K. Dietmayer, "The ADUULM-Dataset - a semantic segmentation dataset for sensor fusion," in *Proceedings of the British Machine Vision Conference (BMVC)*, 2020. 3

[58] D. Dai, C. Sakaridis, S. Hecker, and L. Van Gool, "Curriculum model adaptation with synthetic and real data for semantic foggy scene understanding," *International Journal of Computer Vision*, vol. 128, no. 5, pp. 1182–1204, 2020. 3, 6

[59] F. Tung, J. Chen, L. Meng, and J. J. Little, "The Raincouver scene parsing benchmark for self-driving in adverse weather and at night," *IEEE Robotics and Automation Letters*, vol. 2, no. 4, pp. 2188–2193, 2017. 3, 6

[60] O. Zendel, M. Schörghuber, B. Rainer, M. Murschitz, and C. Beleznai, "Unifying panoptic segmentation for autonomous driving," in *Proceedings of the IEEE/CVF Conference on Computer Vision and Pattern Recognition (CVPR)*, 2022. 3

[61] M. Alibeigi, W. Ljungbergh, A. Tonderski, G. Hess, A. Lilja, C. Lindström, D. Motorniuk, J. Fu, J. Widahl, and C. Petersson, "Zenseact Open Dataset: A large-scale and diverse multimodal dataset for autonomous driving," in *ICCV*, 2023. 3

[62] J. Mei, A. Z. Zhu, X. Yan, H. Yan, S. Qiao, L.-C. Chen, and H. Kretzschmar, "Waymo Open Dataset: Panoramic video panoptic segmentation," in *ECCV*, 2022. 3

[63] J. Long, E. Shelhamer, and T. Darrell, "Fully convolutional networks for semantic segmentation," in *Proceedings of the IEEE Conference on Computer Vision and Pattern Recognition (CVPR)*, June 2015. 3

[64] L.-C. Chen, G. Papandreou, I. Kokkinos, K. Murphy, and A. Yuille, "Semantic image segmentation with deep convolutional nets and fully connected CRFs," in *International Conference on Learning Representations*, May 2015. 3

[65] L.-C. Chen, G. Papandreou, I. Kokkinos, K. Murphy, and A. L. Yuille, "DeepLab: Semantic image segmentation with deep convolutional nets, atrous convolution, and fully connected CRFs," *IEEE Transactions on Pattern Analysis and Machine Intelligence*, vol. 40, no. 4, pp. 834–848, 2018. 3, 6, 7, 8, 9, 10, 13

[66] F. Yu and V. Koltun, "Multi-scale context aggregation by dilated convolutions," in *International Conference on Learning Representations*, 2016. 3

[67] O. Ronneberger, P. Fischer, and T. Brox, "U-Net: Convolutional networks for biomedical image segmentation," in *Medical Image Computing and Computer-Assisted Intervention – MICCAI 2015*, 2015, pp. 234–241. 3

[68] G. Lin, A. Milan, C. Shen, and I. Reid, "RefineNet: Multi-path refinement networks with identity mappings for high-resolution semantic segmentation," in *IEEE Conference on Computer Vision and Pattern Recognition (CVPR)*, 2017. 3, 7, 10, 13

[69] T. Pohlen, A. Hermans, M. Mathias, and B. Leibe, "Full-resolution residual networks for semantic segmentation in street scenes," in *Proceedings of the IEEE Conference on Computer Vision and Pattern Recognition (CVPR)*, July 2017. 3

[70] H. Zhao, J. Shi, X. Qi, X. Wang, and J. Jia, "Pyramid scene parsing network," in *The IEEE Conference on Computer Vision and Pattern Recognition (CVPR)*, 2017. 3

[71] C. Yu, J. Wang, C. Peng, C. Gao, G. Yu, and N. Sang, "BiSeNet: Bilateral segmentation network for real-time semantic segmentation," in *Proceedings of the European Conference on Computer Vision (ECCV)*, September 2018. 3

[72] D. Xu, W. Ouyang, X. Wang, and N. Sebe, "PAD-Net: Multi-tasks guided prediction-and-distillation network for simultaneous depth estimation and scene parsing," in *Proceedings of the IEEE Conference on Computer Vision and Pattern Recognition (CVPR)*, June 2018. 3

[73] T.-W. Ke, J.-J. Hwang, Z. Liu, and S. X. Yu, "Adaptive affinity fields for semantic segmentation," in *Proceedings of the European Conference on Computer Vision (ECCV)*, September 2018. 3

[74] L.-C. Chen, Y. Zhu, G. Papandreou, F. Schroff, and H. Adam, "Encoder-decoder with atrous separable convolution for semantic image segmentation," in *The European Conference on Computer Vision (ECCV)*, September 2018. 3, 10, 11, 13

[75] Z. Zhu, M. Xu, S. Bai, T. Huang, and X. Bai, "Asymmetric non-local neural networks for semantic segmentation," in *Proceedings of the IEEE/CVF International Conference on Computer Vision (ICCV)*, October 2019. 3

[76] J. Fu, J. Liu, H. Tian, Y. Li, Y. Bao, Z. Fang, and H. Lu, "Dual attention network for scene segmentation," in *Proceedings of the IEEE/CVF Conference on Computer Vision and Pattern Recognition (CVPR)*, June 2019. 3, 13

[77] Z. Huang, X. Wang, L. Huang, C. Huang, Y. Wei, and W. Liu, "CCNet: Criss-cross attention for semantic segmentation," in *Proceedings of the IEEE/CVF International Conference on Computer Vision (ICCV)*, October 2019. 3

[78] J. Wang, K. Sun, T. Cheng, B. Jiang, C. Deng, Y. Zhao, D. Liu, Y. Mu, M. Tan, X. Wang, W. Liu, and B. Xiao, "Deep high-resolution representation learning for visual recognition," *IEEE Transactions on Pattern Analysis and Machine Intelligence*, 2020. 3, 10, 13

[79] Y. Yuan, X. Chen, and J. Wang, "Object-contextual representations for semantic segmentation," in *The European Conference on Computer Vision (ECCV)*, 2020, pp. 173–190. 3

[80] J. Hoffman, D. Wang, F. Yu, and T. Darrell, "FCNs in the wild: Pixel-level adversarial and constraint-based adaptation," *arXiv e-prints*, vol. abs/1612.02649, December 2016. 3

[81] X. Lai, Z. Tian, X. Xu, Y. Chen, S. Liu, H. Zhao, L. Wang, and J. Jia, "DecoupleNet: Decoupled network for domain adaptive semantic segmentation," in *European Conference on Computer Vision (ECCV)*, 2022. 3

[82] R. Li, S. Li, C. He, Y. Zhang, X. Jia, and L. Zhang, "Class-balanced pixel-level self-labeling for domain adaptive semantic segmentation," in *Proceedings of the IEEE/CVF Conference on Computer Vision and Pattern Recognition (CVPR)*, 2022. 3

[83] X. Guo, J. Liu, T. Liu, and Y. Yuan, "SimT: Handling open-set noise for domain adaptive semantic segmentation," in *Proceedings of the IEEE/CVF Conference on Computer Vision and Pattern Recognition (CVPR)*, 2022. 3

[84] F. Shen, A. Gurram, Z. Liu, H. Wang, and A. Knoll, "DiGA: Distil to generalize and then adapt for domain adaptive semantic segmentation," in *Proceedings of the IEEE/CVF Conference on Computer Vision and Pattern Recognition (CVPR)*, 2023. 3

[85] R. Gong, Q. Wang, M. Danelljan, D. Dai, and L. Van Gool, "Continuous pseudo-label rectified domain adaptive semantic segmentation with implicit neural representations," in *Proceedings of the IEEE/CVF Conference on Computer Vision and Pattern Recognition (CVPR)*, 2023. 3

[86] K. He, G. Gkioxari, P. Dollár, and R. Girshick, "Mask r-cnn," in *2017 IEEE International Conference on Computer Vision (ICCV)*, 2017, pp. 2980–2988. 4, 12, 13

[87] M. Hassaballah, M. A. Kenk, K. Muhammad, and S. Minaee, "Vehicle detection and tracking in adverse weather using a deep learning framework," *IEEE Transactions on Intelligent Transportation Systems*, vol. 22, no. 7, pp. 4230–4242, 2021. 6

[88] E. Xie, W. Wang, Z. Yu, A. Anandkumar, J. M. Alvarez, and P. Luo, "SegFormer: Simple and efficient design for semantic segmentation with transformers," in *Advances in Neural Information Processing Systems*, 2021. 6, 7, 8, 9

[89] W. Tranheden, V. Olsson, J. Pinto, and L. Svensson, "DACS: Domain adaptation via cross-domain mixed sampling," in *Proceedings of the IEEE/CVF Winter Conference on Applications of Computer Vision (WACV)*, 2021. 7

[90] S. Ren, K. He, R. Girshick, and J. Sun, "Faster R-CNN: Towards real-time object detection with region proposal networks," in *Advances in Neural Information Processing Systems*, 2015, pp. 91–99. 8, 9

[91] Z. Tian, C. Shen, H. Chen, and T. He, "FCOS: A simple and strong anchor-free object detector," in *IEEE T. Pattern Analysis and Machine Intelligence (TPAMI)*, 2021. 8, 9

[92] B. Cheng, I. Misra, A. G. Schwing, A. Kirillov, and R. Girdhar, "Masked-attention mask transformer for universal image segmentation," in *CVPR*, 2022. 10, 11, 12, 13

[93] Z. Chen, Y. Duan, W. Wang, J. He, T. Lu, J. Dai, and Y. Qiao, "Vision transformer adapter for dense predictions," *arXiv preprint arXiv:2205.08534*, 2022. 10

[94] A. Kirillov, R. Girshick, K. He, and P. Dollar, "Panoptic feature pyramid networks," in *Proceedings of the IEEE/CVF Conference on Computer Vision and Pattern Recognition (CVPR)*, June 2019. 11, 12, 13

[95] W. Zhang, J. Pang, K. Chen, and C. C. Loy, "K-net: Towards unified image segmentation," in *Advances in Neural Information Processing Systems*, M. Ranzato, A. Beygelzimer, Y. Dauphin, P. Liang, and J. W. Vaughan, Eds., vol. 34. Curran Associates, Inc., 2021, pp. 10 326–10 338. [Online]. Available: https://proceedings.neurips.cc/paper_files/paper/2021/file/55a7cf9c71f1c9c495413f934dd1a158-Paper.pdf 11, 12, 13

[96] B. Cheng, M. D. Collins, Y. Zhu, T. Liu, T. S. Huang, H. Adam, and L.-C. Chen, "Panoptic-deeplab: A simple, strong, and fast baseline for bottom-up panoptic segmentation," in *CVPR*, 2020. 11, 12, 13

[97] Z. Cai and N. Vasconcelos, "Cascade r-cnn: High quality object detection and instance segmentation," *arXiv preprint arXiv:1906.09756*, 2019. 12, 13

[98] K. Chen, J. Pang, J. Wang, Y. Xiong, X. Li, S. Sun, W. Feng, Z. Liu, J. Shi, W. Ouyang, C. C. Loy, and D. Lin, "Hybrid task cascade for instance segmentation," in *IEEE Conference on Computer Vision and Pattern Recognition*, 2019. 12, 13

[99] S. Qiao, L.-C. Chen, and A. Yuille, "Detectors: Detecting objects with recursive feature pyramid and switchable atrous convolution," *arXiv preprint arXiv:2006.02334*, 2020. 12, 13

[100] X. Wu, Z. Wu, H. Guo, L. Ju, and S. Wang, "DANNet: A one-stage domain adaption network for unsupervised nighttime semantic segmentation," in *IEEE/CVF Conference on Computer Vision and Pattern Recognition (CVPR)*, June 2021. 13

[101] P. Bevandić, I. Krešo, M. Oršić, and S. Šegvić, "Simultaneous semantic segmentation and outlier detection in presence of domain shift," in *German Conference on Pattern Recognition*, 2019. 13, 14

[102] A. Kendall and Y. Gal, "What uncertainties do we need in Bayesian deep learning for computer vision?" in *Advances in Neural Information Processing Systems*, 2017. 13

Christos Sakaridis is a lecturer at ETH Zürich and a senior postdoctoral researcher at Computer Vision Lab of ETH Zürich. His research fields are computer vision, machine learning, and artificial intelligence. The focus of his research is on semantic and geometric visual perception, involving multiple domains, visual conditions, and modalities. Since 2021, he is the Principal Engineer of TRACE-Zürich, a large-scale project on computer vision for autonomous cars and robots. He received the ETH Zurich Career Seed Award in 2022. He obtained his PhD from ETH Zürich in 2021, having worked in Computer Vision Lab. Prior to that, he received his MSc in Computer Science from ETH Zürich in 2016 and his Diploma in Electrical and Computer Engineering from National Technical University of Athens in 2014.

Haoran Wang is a PhD student at Max Planck Institute for Informatics. He received his M.Sc degree from ETH Zürich in 2020 and B.Eng degree from Sichuan University in 2017. He has served as a reviewer for major computer vision conferences and journals (e.g. CVPR, ICCV, ECCV, IEEE T-PAMI). His research interests include machine learning and computer vision, especially transfer learning and domain adaptation.

Ke Li has finished her PhD study in computer vision from ETH Zurich, in 2024. Before that, she has obtained her Bachelor's degree in Clinical Medicine from Tongji Medical School, Huazhong University of Science and Technology, China, in 2011. She then obtained her Master's degree in gene expression analysis from the University of Basel, in 2015, and her Master's degree in Biostatistics from the University of Zurich, in 2018. Her current research interests lie in Hyperspectral Imaging, Hyperspectral Image Super-resolution, Learning with Auxiliary Tasks, and Domain Adaptation.

René Zurbrügg is a PhD student at the ETH AI Center and part of the Robotic Systems Lab (RSL) and Computer Vision and Geometry Group (CVG). He received his M.Sc degree in Robotics, Systems and Control from ETH Zürich in 2022 and his B.Sc degree in Information Technology and Electrical Engineering in 2021 from ETH Zürich. His research interests lie in the field of embodied intelligence, mainly focusing on the interconnection of computer vision and robotics applied to interactive tasks such as manipulation and active exploration.

Arpit Jadon is an AI Research Engineer at Max Planck Institute for Informatics (MPII). He graduated with a Master's degree in Computer Science from Saarland University in 2023. He obtained his Bachelor's degree in Electrical Engineering from Aligarh Muslim University in 2019, where he was also awarded for excellent holistic performance in academics and research. For his Master's thesis, he worked on semantic road scene understanding with realistic synthetic data. His primary research interests revolve around computer vision and machine learning, with a special focus on domain adaptation and synthetic data generation for autonomous driving.

Wim Abbeloos obtained a Master of Science in applied engineering at University of Antwerp in 2011. He then worked as a researcher and PhD student at the Industrial Vision Lab (InViLab) at University of Antwerp and the Embedded and Artificially Intelligent Vision Engineering group (EAVISE) at KU Leuven, working on 3D object detection and pose estimation for robotics applications. During an internship at Mitsubishi Electric Research Laboratories in 2017 he worked on the problem of unsupervised 3D object discovery. Subsequently, he joined Toyota Motor Europe (Belgium) in 2018, where he currently coordinates and manages research collaborations with top research institutes in Europe in the fields of computer vision and artificial intelligence, including automated driving and other application areas. Additionally, he supports the transfer and integration of the developed knowledge into future applications and products.

Daniel Olmeda Reino received the PhD degree from UC3M, Spain, in 2014, in the field of computer vision. He joined Toyota Motor Europe in 2015, where he currently is a Technical Manager in the AI division. His research interests are in computer vision and machine learning. His latest work is on semi-supervised and continual learning, visual tracking and prediction, novelty detection, domain adaptation, visual localization, and robust perception among others.

Luc Van Gool is a full professor for Computer Vision at ETH Zürich, the KU Leuven and INSAIT. He leads research and/or teaches at all three institutions. He has authored over 900 papers. He has been a program committee member of several major computer vision conferences (e.g. Program Chair ICCV'05, Beijing, General Chair of ICCV'11, Barcelona, and of ECCV'14, Zürich). His main interests include 3D reconstruction and modeling, object recognition, and autonomous driving. He received several best paper awards (e.g. David Marr Prize '98, Best Paper CVPR'07). He received the Koenderink Award in 2016 and the "Distinguished Researcher" nomination by the IEEE Computer Society in 2017. In 2015 he also received the 5-yearly Excellence Prize by the Flemish Fund for Scientific Research. He was the holder of an ERC Advanced Grant (VarCity). Currently, he leads computer vision research for autonomous driving in the context of the Toyota TRACE labs at ETH and in Leuven, and has an extensive collaboration with Huawei on the topic of image and video enhancement.

Dengxin Dai has received his PhD degree in computer vision from ETH Zürich, in 2016. He is now the Director of Research with Huawei Zürich Research Center. Before that, he was a senior group leader with the Max Planck Institute for Informatics and a senior scientist with ETH Zürich. He is a member of the ELLIS Society. He has organized multiple well-received workshops, is currently an associate editor of the International Journal of Computer Vision, and has been area chair of multiple vision conferences including CVPR, ECCV, and ICRA. He received the Golden Owl Award with ETH Zürich in 2021 for his exceptional teaching and received the German Pattern Recognition Award in 2022 for his outstanding scientific contribution in the area of scalable and robust visual perception.